WFU Physics Colloquium on

First Principles Investigations of Electrolyte Materials in All-Solid-State Batteries

Yan Li

Department of Physics, Wake Forest University

Thursday, November 4, 2021

Wake Forest University

WAKE FOREST UNIVERSITY

Outline

- ❑ Research background: General motivation and theoretical tools
- ❑ Finished/ongoing projects: Inputs and outcomes

$Na_4P_2S_6$, $Li_4P_2S_6$, and possible alloy

Yan Li, Zachary D. Hood, and N. A. W. Holzwarth

Phys. Rev. Mater. 4, 045406 (2020)

Phonon dispersion

Yan Li, W. C. Kerr, and N. A. W. Holzwarth

J. Condens. Matter Phys. 32, 055402 (2020)

Li_3BO_3 and Li_3BN_2 (I & II)

Yan Li, Zachary D. Hood, and N. A. W. Holzwarth

Phys. Rev. Mater. 5, 085402 & 085403 (2021)

$Li_{4+x}B_7O_{12+x/2}Cl$ (x = 0, 1) and related

$Li_{7.5}B_{10}S_{18}X_{1.5}$ (X = Cl, Br, I)

Outline

- ❑ **Research background: General motivation and theoretical tools**
- ❑ **Finished/ongoing projects: Inputs and outcomes**

$Na_4P_2S_6$, $Li_4P_2S_6$, and possible alloy

Yan Li, Zachary D. Hood, and N. A. W. Holzwarth

Phys. Rev. Mater. 4, 045406 (2020)

Phonon dispersion

Yan Li, W. C. Kerr, and N. A. W. Holzwarth

J. Condens. Matter Phys. 32, 055402 (2020)

Li_3BO_3 and Li_3BN_2 (I & II)

Yan Li, Zachary D. Hood, and N. A. W. Holzwarth

Phys. Rev. Mater. 5, 085402 & 085403 (2021)

$Li_{4+x}B_7O_{12+x/2}Cl$ (x = 0, 1) and related

$Li_{7.5}B_{10}S_{18}X_{1.5}$ (X = Cl, Br, I)

Motivation of studying battery materials

❑ Nobel prize recognition

"*The Lithium ion batteries have laid the foundation of a wireless, fossil fuel-free society and are of the greatest benefit to humankind*" (words of the Nobel committee)

❑ Continuous challenges

- More demanding applications
- **New materials and recipes for battery components**
- Balance of capacity, cost, size, and weight

The Nobel Prize in Chemistry 2019

rewards the development of lithium ion battery

John B. Goodenough

M. Stanley Whittingham

Akira Yoshino

Whittingham: developed the first functional lithium battery in the early 1970s
Goodenough: doubled the battery's potential in the following decade
Yoshino: eliminated pure lithium from the battery, making it much safer to use

Photo from https://www.nobelprize.org

Components of a rechargeable Li ion battery

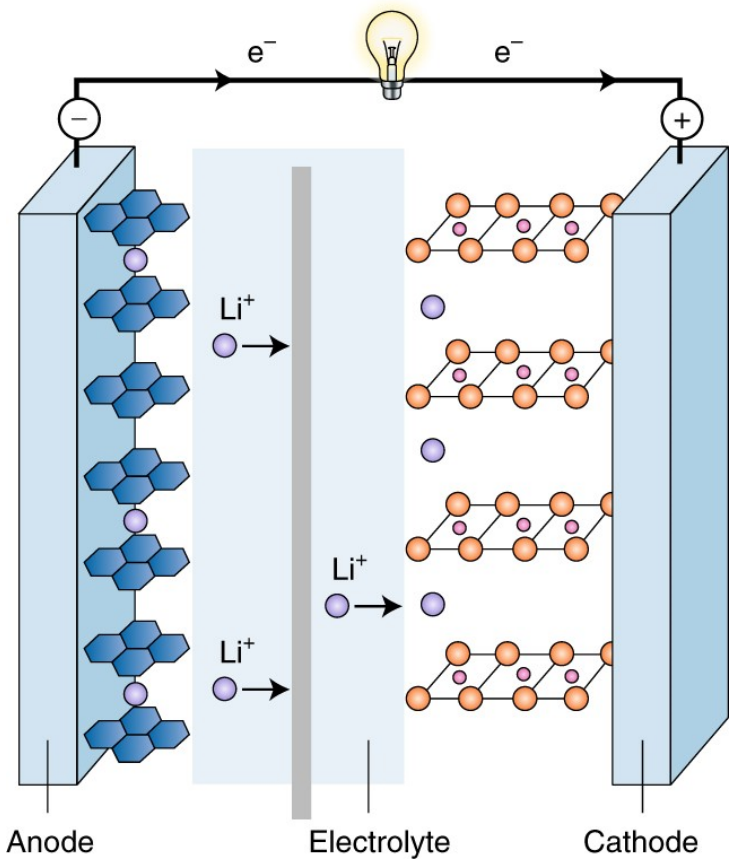

Discharge mode

Role of the electrolyte:

Allow for the transport of Li ions, excluding electrons from the battery and forcing them through the external circuit.

Why solid-state electrolyte?

- Superior safety due to the absence of flammable liquid content
- Excellent physical and chemical stability
- Compatible and stable with Li metal anodes
- Acceptable ionic conductivity

How can computer modeling help ?

For known and theoretically predicted Li or Na ion solid electrolyte materials (electronically insulating & operate in ground electronic states)

- ❑ Structures and stabilities
  - Construct models for various forms of ideal crystals
  - Simulate the static and vibrational properties
  - Identify stable and metastable configurations
- ❑ Electrolyte properties
  - Mechanisms: vacancy migration, interstitial migration
  - Quantitative analysis: defect formation energy, migration energy barrier, ionic conductivity
  - Model ideal electrolyte interfaces with anodes

Many-body Schrödinger equation

Exact time-independent Schrödinger equation for a system of *N* electrons with coordinates $\{\boldsymbol{r}_i\}$ $(i = 1, 2, \cdots, N)$ and *M* nuclei with coordinates $\{\boldsymbol{R}_I\}$ $(I = 1, 2, \cdots, M)$

$$i\frac{\partial}{\partial t}\Psi(\{\mathbf{r}_i\},\{\mathbf{R}_I\}) = \hat{H}_{\text{tot}}\ \Psi(\{\mathbf{r}_i\},\{\mathbf{R}_I\})$$

where $\hat{H}_{\text{tot}} = -\sum_I \frac{\hbar^2}{2M_I}\nabla_I^2 + \frac{e^2}{2}\sum_{I\neq J}\frac{Z_I Z_J}{|\mathbf{R}_I - \mathbf{R}_J|}$

$\hat{T}_{\text{N}}(\mathbf{R}) + \hat{V}_{\text{NN}}(\mathbf{R})$
Nuclear

$$-\frac{\hbar^2}{2m}\sum_i \nabla_i^2 + \frac{e^2}{2}\sum_{i\neq j}\frac{1}{|\mathbf{r}_i - \mathbf{r}_j|}$$

$\hat{T}_{\text{e}}(\mathbf{r}) + \hat{V}_{\text{ee}}(\mathbf{r})$
Electronic

$$-\sum_{i,I}\frac{Z_I e^2}{|\mathbf{r}_i - \mathbf{R}_I|}$$

$\hat{V}_{\text{eN}}(\mathbf{r},\mathbf{R})$
Mixed

First principles methods: a series of well-established physical approximations

Born-Oppenheimer approximation

Born-Oppenheimer approximation ($M_I \gg m$)

$$\Psi(\{\mathbf{r}_i\},\{\mathbf{R}_I\}) = \Psi_{\mathbf{R}}(\{\mathbf{r}_i\})\chi(\{\mathbf{R}_I\})$$

Electron part: treated quantum mechanically

Nuclei part: treated classically

Electronic Schrödinger equation:

$$\hat{H}_{\mathbf{R}}\Psi_{\mathbf{R}}(\{\mathbf{r}_i\}) = E_{\mathbf{R}}\Psi_{\mathbf{R}}(\{\mathbf{r}_i\})$$

$$\hat{H}_{\mathbf{R}} = -\frac{\hbar^2}{2m}\sum_i \nabla_i^2 - \sum_{i,I}\frac{Z_I e^2}{|\mathbf{r}_i - \mathbf{R}_I|} + \frac{e^2}{2}\sum_{i\neq j}\frac{1}{|\mathbf{r}_i - \mathbf{r}_j|}$$

Density functional theory and numerical schemes

Hohenberg-Kohn theorem:

$$E_{\mathbf{R}} = F[\rho(\mathbf{r})]$$ Reduction of dimensionality (3N → 3)!

Kohn-Sham equations:

$$E_{\mathbf{R}} = F[\rho(\mathbf{r})] = E_{\mathbf{T}} + E_{\text{ext}} + E_{\mathbf{H}} + E_{\mathbf{xc}}$$

$E_{\mathbf{xc}}$: unknown

$E_{\mathbf{T}}$, E_{ext}, $E_{\mathbf{H}}$: obtained from independent electrons approximation

$$\left.\frac{\delta F[\rho]}{\delta \rho}\right|_{\rho_0} = 0$$

Hohenberg and Kohn, *Phys. Rev.* **136**, B864 (1964)
Kohn and Sham, *Phys. Rev.* **140**, A1133 (1965)

$$\left[-\frac{\hbar^2}{2m}\nabla^2 + V_{\text{ext}}(\mathbf{r}) + V_{\text{H}}(\mathbf{r}) + V_{xc}(\mathbf{r})\right]\psi_i(\mathbf{r}) = \varepsilon_i\psi_i(\mathbf{r})$$

$$V_{\text{ext}}(\mathbf{r}) = -\sum_I \frac{Z_I e^2}{|\mathbf{r} - \mathbf{R}_I|} \qquad \nabla^2 V_{\text{H}}(\mathbf{r}) = -4\pi e^2 \rho(\mathbf{r}) \qquad V_{\text{xc}}(\mathbf{r}) = \left.\frac{\delta E_{\text{xc}}[\rho]}{\delta \rho}\right|_{\rho(\mathbf{r})}$$

$$\rho(\mathbf{r}) = \sum_i |\psi_i(\mathbf{r})|^2$$

LDA: Perdew and Wang, Phys. Rev. B **45**, 13244 (1992)
GGA: Perdew et al., Phys. Rev. L **77**, 3865 (1996)
…

To solve DFT equations: Planewave representations; Pseudopotential formulations

Output of DFT calculations

At equilibrium:

$$\mathbf{F}_I = -\frac{\partial U(\{\mathbf{R}_I\})}{\partial \mathbf{R}_I} = 0$$

- Optimized structural parameters
- Static lattice energy: $U_{\mathrm{SL}} = \min U(\{\mathrm{R_I}\})$
- Kohn-Sham orbitals and energies
- Interstitial-vacancy pair formation energy: $E_{\mathrm{f}} = U_{\mathrm{SL}}^{\mathrm{defect}} - U_{\mathrm{SL}}^{\mathrm{perfect}}$
- Ionic migration energies: E_{m}

Lattice vibrations in crystalline solids

Near equilibrium (Harmonic approximation):

$$U(\{\mathbf{u}_s(l)\})_{harm} = U(\{\mathbf{u}_s(l)\}=0) + \frac{1}{2}\sum_{ls\alpha}\sum_{mt\beta} C_{st}^{\alpha\beta}(l,m)u_{s\alpha}(l)u_{t\beta}(m) \quad \text{where} \quad C_{st}^{\alpha\beta}(l,m) = \left.\frac{\partial^2 U}{\partial u_s^{\alpha}(l)\partial u_t^{\beta}(m)}\right|_0$$

$$M_s(\omega^{\nu})^2 u_{s\alpha}^{\nu}(\mathbf{q}) = \sum_{t\beta}\tilde{C}_{st}^{\alpha\beta}(\mathbf{q})u_{t\beta}^{\nu}(\mathbf{q})$$

First principles phonon calculations:
Density functional perturbation theory (DFPT)

- Phonon frequencies and eigenvectors at any wavevector
- Phonon dispersions: $\omega^{\nu} \sim \mathbf{q}$ *(by specifying a path of high symmetry points)*
- Phonon density of states (PDOS): $g(\omega) = \frac{V}{(2\pi)^3}\int d^3q \sum_{\nu=1}^{3N}\delta(\omega-\omega^{\nu}(\mathbf{q}))$
- Thermodynamic properties such as the vibrational energy: $F_{vib}(T) = k_B T\int_0^{\infty} d\omega \ln\left(2\sinh\left(\frac{\hbar\omega}{2k_BT}\right)\right)g(\omega)$

Combined the DFT and DPFT energies

- The Helmholtz free energy: $F(T) = F_{SL}(T) + F_{vib}(T) \approx U_{SL} + F_{vib}(T)$

Ordered system with constant volume

DFT DFPT

Li/Na ions diffusion mechanisms

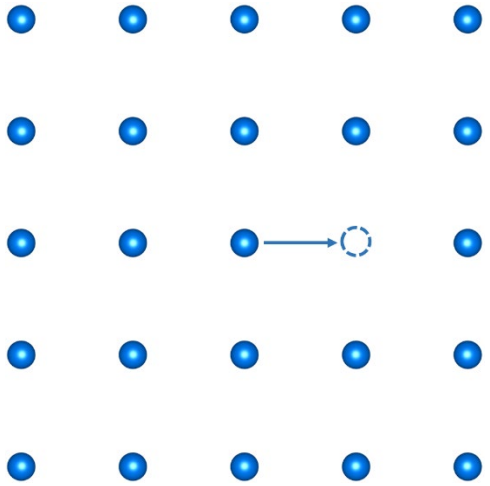

Vacancy mechanism

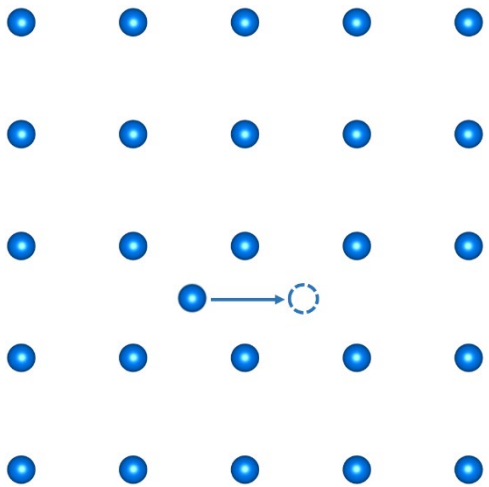

Interstitial mechanism

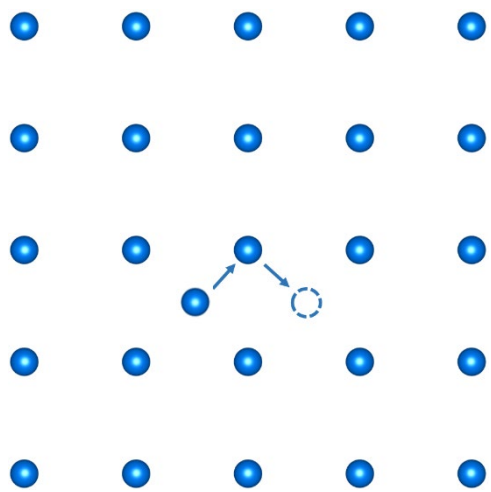

Interstitialcy (kick-out) mechanism

High ionic diffusivity in solid conductors requires:

- Rigid framework and high concentration of mobile ions
- Sufficient number of available sites for the mobile ions to occupy
- Continuous channels with low migration barrier energies

Numerical methods for studying ionic migrations

Nudged Elastic Band (NEB)

Requires a specific migration pathway as input

Simple but limited

Picture credit to Prof. Holzwarth

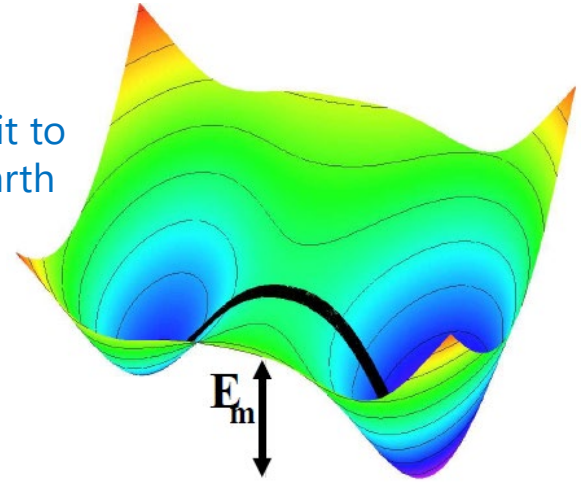

For perfect crystals: $E_a^{\mathrm{NEB}} = E_m^{\mathrm{NEB}} + \frac{1}{2}E_f$

Arrhenius relation: $\sigma(T) = \frac{A}{T} e^{-E_a^{\mathrm{NEB}}/k_B T}$

Ab Initio Molecular Dynamics (AIMD)

Statistical averaging over all diffusional events

Large supercell & long simulation time

$$\mathrm{MSD}(t,T) \equiv \frac{1}{N_{\mathrm{a}}} \left\langle \sum_{i=1}^{N_{\mathrm{a}}} |\mathbf{R}_i(t) - \mathbf{R}_i(0)|^2 \right\rangle$$

$$D_{tr}(T) = \frac{1}{6} \lim_{t\to\infty} \frac{1}{(t - t_{eq})} \mathrm{MSD}(t - t_{eq}, T)$$

$$D_{\mathrm{tr}}(T) = D_0 e^{-E_a^{\mathrm{MD}}/k_B T}$$

Nernst-Einstein relation:

$$\sigma(T) = \frac{N}{V}\frac{q^2}{k_B T} D_{\mathrm{all}} = \frac{1}{H_r}\frac{N}{V}\frac{q^2}{k_B T} D_{\mathrm{tr}}$$

Haven ratio: $H_r = D_{\mathrm{tr}}/D_{\mathrm{all}}$

measures effects of correlated motions

Summary of computational methods

- Density Functional Theory (DFT) and Density Functional Perturbation Theory (DFPT) with the modified Perdew-Burke-Ernzerhof generalized gradient approximation **(PBEsol GGA)**

  Perdew *et al.*, *PRL* **100**, 136406 (2008)

- The projector augmented wave (PAW) formalism with atomic datasets generated by **ATOMPAW** code available at http://pwpaw.wfu.edu

- First principles electronic-structure calculations and materials modeling

  https://www.abinit.org/

  https://www.quantum-espresso.org/

- Structural visualization, symmetry identification, X-ray patterns

  https://jp-minerals.org/vesta/

  http://www.xcrysden.org/

  https://stokes.byu.edu/iso/findsym.php

  https://www.ccdc.cam.ac.uk/solutions/csd-core/components/mercury/

Outline

- Research background: General motivation and theoretical tools
- **Finished/ongoing projects: Inputs and outcomes**

$Na_4P_2S_6$, $Li_4P_2S_6$, and possible alloy

Yan Li, Zachary D. Hood, and N. A. W. Holzwarth

Phys. Rev. Mater. 4, 045406 (2020)

Phonon dispersion

Yan Li, W. C. Kerr, and N. A. W. Holzwarth

J. Condens. Matter Phys. 32, 055402 (2020)

Li_3BO_3 and Li_3BN_2 (I & II)

Yan Li, Zachary D. Hood, and N. A. W. Holzwarth

Phys. Rev. Mater. 5, 085402 & 085403 (2021)

$Li_{4+x}B_7O_{12+x/2}Cl$ (x = 0, 1) and related

$Li_{7.5}B_{10}S_{18}X_{1.5}$ (X = Cl, Br, I)

Outline

- Research background: General motivation and theoretical tools
- **Finished/ongoing projects: Inputs and outcomes**

$Na_4P_2S_6$, $Li_4P_2S_6$, and possible alloy

Yan Li, Zachary D. Hood, and N. A. W. Holzwarth

Phys. Rev. Mater. 4, 045406 (2020)

Phonon dispersion

Yan Li, W. C. Kerr, and N. A. W. Holzwarth

J. Condens. Matter Phys. 32, 055402 (2020)

Li_3BO_3 and Li_3BN_2 (I & II)

Yan Li, Zachary D. Hood, and N. A. W. Holzwarth

Phys. Rev. Mater. 5, 085402 & 085403 (2021)

$Li_{4+x}B_7O_{12+x/2}Cl$ (x = 0, 1) and related

$Li_{7.5}B_{10}S_{18}X_{1.5}$ (X = Cl, Br, I)

Li Boracites

Mineral boracites $\mathbf{M_3B_7O_{13}X}$, where M = Mg, Cr, Mn, Fe, Co, Ni, Zn or Cd, and X = Cl, Br or I

Li-containing boracites $\mathbf{Li_{4+x}B_7O_{12+x/2}X}$, where $0 \leq x \leq 1$, and X = Cl, Br or I

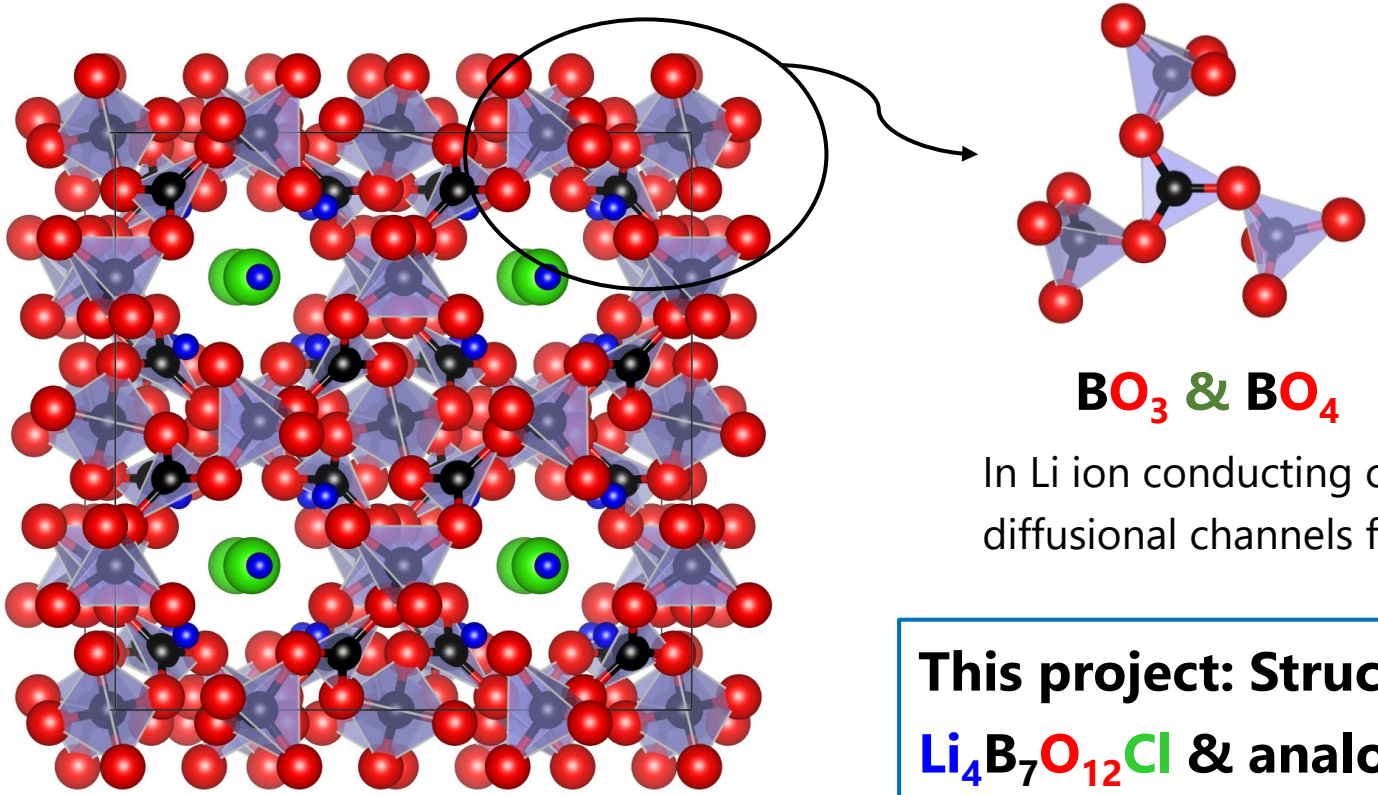

BO_3 & BO_4

In Li ion conducting compounds, the **Li** ions are arranged in diffusional channels formed by the $\mathbf{B_7O_{12}}$ framework.

This project: Structural and electrolyte properties of $Li_4B_7O_{12}Cl$ & analogs obtained by ionic substitutions

Reported structures of $Li_4B_7O_{12}Cl$ from 1977*

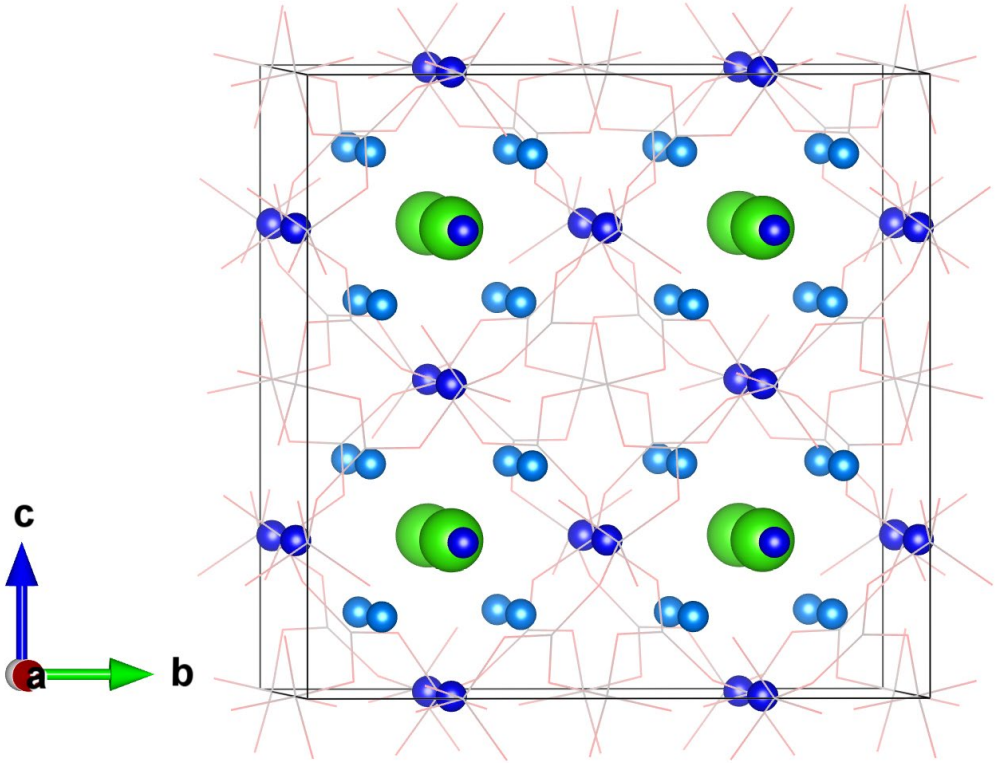

Ideal cubic model

8 formula units/cell

Three disordered phases

*Jeitschko *et al.*, *Acta Cryst.* B33, 2767-2775 (1977)

Above 348 K — **γ phase ($F\bar{4}3c$, No. 219)**
Li(24c): 93.7% occupied
Li(32e): 31.6% occupied

310 – 348 K — **β phase ($P\bar{4}3c$, No. 218)**
Ideal $F\bar{4}3c$ model
Li(24c): 96.7% occupied
Li(32e): 27.8% occupied

Room T — **α phase (Exp. R3, No. 146)**
Ideal $F\bar{4}3c$ model
Li(24c): 100% occupied
Li(32e): 25% occupied

* The real space groups of the α and β phases are subgroups of $F\bar{4}3c$.

** The atomic positions for both α and β phases are not known in experiment.

Find the ground state structure for α-$Li_4B_7O_{12}Cl$

Li(24c) Li(32e) B O Cl

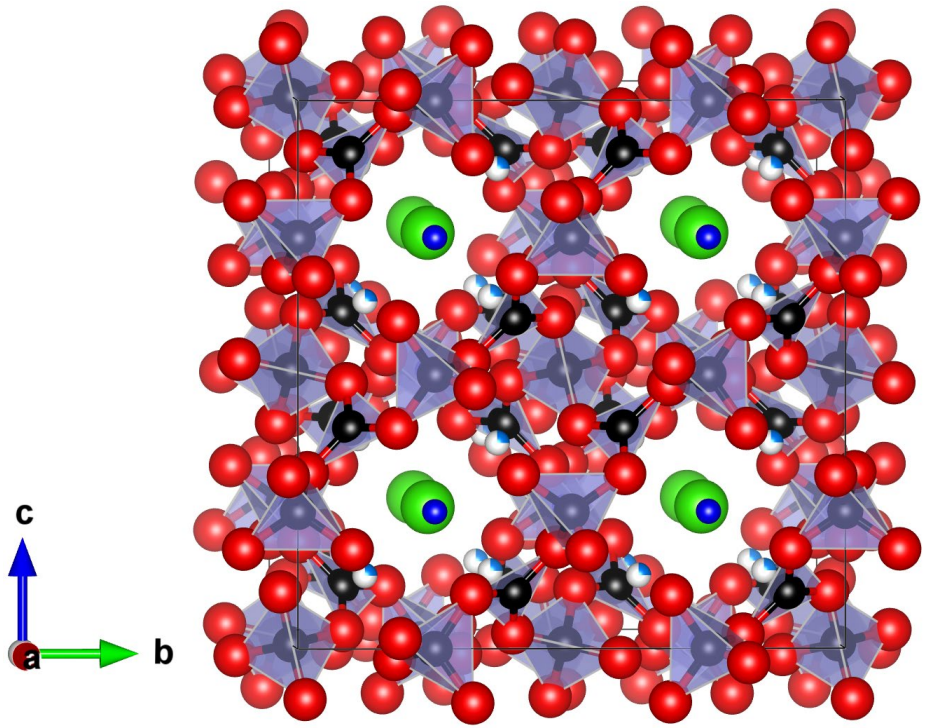

Conventional cell of F$\bar{4}$3c model

Li(24c): 100% occupied

Li(32e): 25% occupied

Perform geometry optimizations for 28 (C_8^2) unique configurations in the primitive cell setting

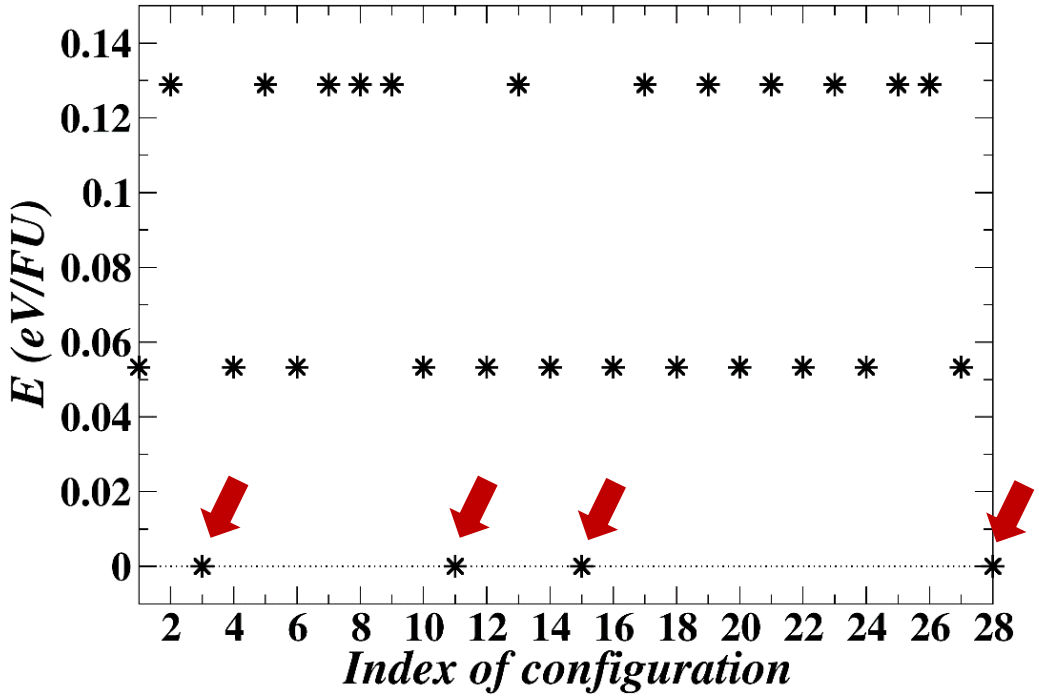

The calculation finds four identical lowest-energy configurations with the **rhombohedral R3c (No. 161)** symmetry

α-$Li_4B_7O_{12}Cl$ in rhombohedral R3c structure

Conventional cell
8 formula units

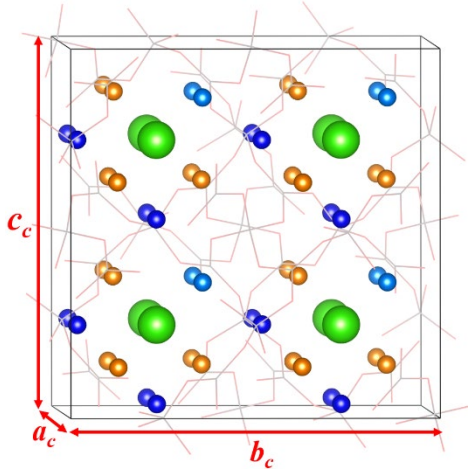

Host Li sites
B-O Wireframe
Native Li vacancies
Cl

Face-centered primitive cell
2 formula units

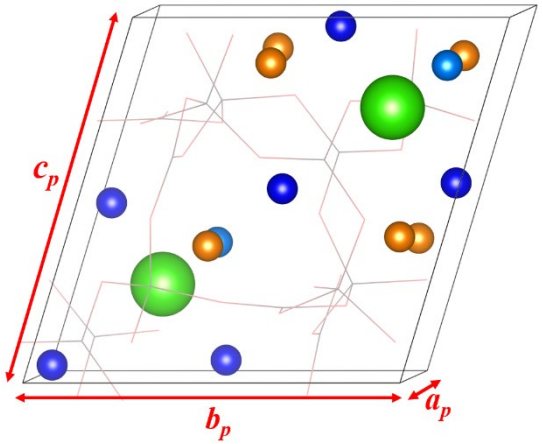

$\mathbf{a_c} = a_c(\hat{\mathbf{x}}(\lambda_c + 2\mu_c) + \hat{\mathbf{y}}(\lambda_c - \mu_c) + \hat{\mathbf{z}}(\lambda_c - \mu_c))$
$\mathbf{b}_c = a_c(\hat{\mathbf{x}}(\lambda_c - \mu_c) + \hat{\mathbf{y}}(\lambda_c + 2\mu_c) + \hat{\mathbf{z}}(\lambda_c - \mu_c))$
$\mathbf{c_c} = a_c(\hat{\mathbf{x}}(\lambda_c - \mu_c) + \hat{\mathbf{y}}(\lambda_c - \mu_c) + \hat{\mathbf{z}}(\lambda_c + 2\mu_c))$

$$\lambda_c \equiv \frac{\sqrt{1+2\cos\theta_c}}{3} \text{ and } \mu_c \equiv \frac{\sqrt{1-\cos\theta_c}}{3}$$

$$\cos(\theta_c) = \frac{2\cos(\theta_p) - 1}{3 - 2\cos(\theta_p)}$$

$a_c = b_c = c_c$ and $\alpha = \beta = \gamma = \theta_c \approx 90°$

$\mathbf{a_p} = (\mathbf{a_c} + \mathbf{b_c})/2 = a_p(\hat{\mathbf{x}}(\lambda_p + \mu_p) + \hat{\mathbf{y}}(\lambda_p + \mu_p) + \hat{\mathbf{z}}(\lambda_p - 2\mu_p))$
$\mathbf{b_p} = (\mathbf{b_c} + \mathbf{c_c})/2 = a_p(\hat{\mathbf{x}}(\lambda_p - 2\mu_p) + \hat{\mathbf{y}}(\lambda_p + \mu_p) + \hat{\mathbf{z}}(\lambda_p + \mu_p))$
$\mathbf{c_p} = (\mathbf{a_c} + \mathbf{c_c})/2 = a_p(\hat{\mathbf{x}}(\lambda_p + \mu_p) + \hat{\mathbf{y}}(\lambda_p - 2\mu_p) + \hat{\mathbf{z}}(\lambda_p + \mu_p))$

$$\lambda_p \equiv \frac{\sqrt{1+2\cos\theta_p}}{3} \text{ and } \mu_p \equiv \frac{\sqrt{1-\cos\theta_p}}{3} \text{ and } a_p = \frac{a_c}{\sqrt{3-2\cos(\theta_p)}}$$

$$\cos(\theta_p) = \frac{1+3\cos(\theta_c)}{2(1+\cos(\theta_c))}$$

$a_p = b_p = c_p$ and $\alpha = \beta = \gamma = \theta_p \approx 60°$

α-$Li_4B_7O_{12}Cl$ in rhombohedral R3c structure

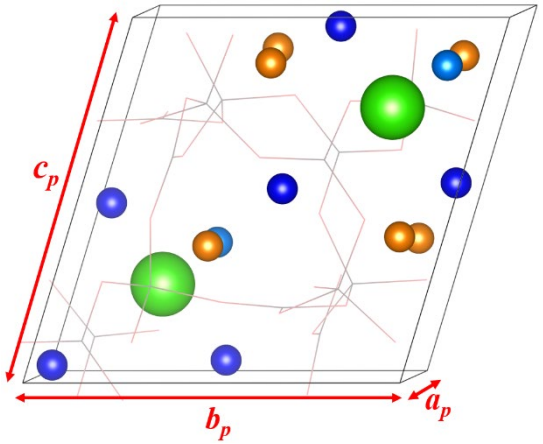

Primitive cell model

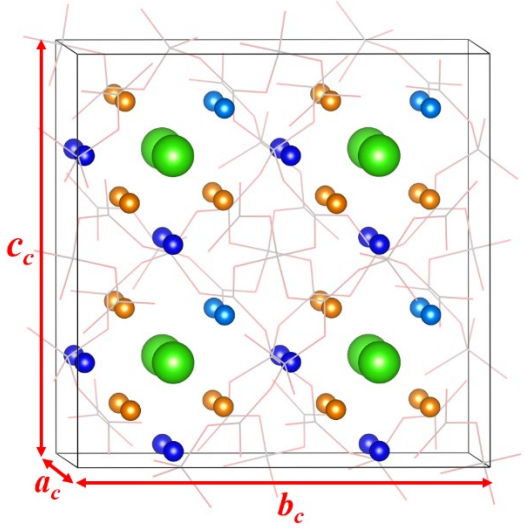

Conventional cell model

Lattice parameters and Li ion fractional coordinates for the R3c structure of α-$Li_4B_7O_{12}Cl$, comparing calculated results with the experimental measurements.

$Li_4B_7O_{12}Cl$	a = b = c (Å)	α= β = γ (deg)
Cal. R3c	12.137	90.108
Exp.* R3	12.141	90.084
Exp.* F$\bar{4}$3c model	12.141	90.000

Cal. R3c				Exp. F$\bar{4}$3c model			
Atom	Wyck	f(x, y, z) (conv.)	Occ.	Atom	Wyck	f(x, y, z)	Occ.
Li(1)	4x6 b	(0.030, 0.245, 0.245)	1.00	Li(1)	24 c	(0.000, 0.250, 0.250)	1.00
Li(2)	4x2 a	(0.865, 0.865, 0.865)	1.00	Li(2)	32 e	(0.871, 0.871, 0.871)	0.25
Vac. Li	4x6 b	(0.633, 0.635, 0.873)	0.00				

*Experimental data taken from Jeitschko *et al.*, *Acta Cryst.* B. **33**, 2767-2775 (1977)

Phase stability of α-$Li_4B_7O_{12}Cl$

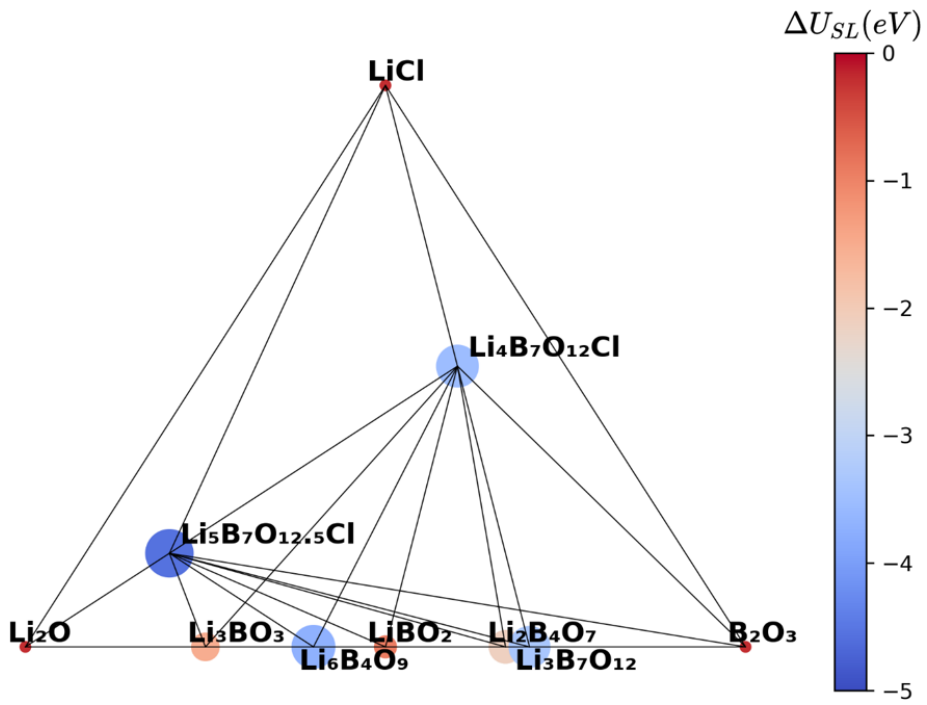

Li_2O-B_2O_3-LiCl phase diagram at 0 K and 0 atm

Reaction energy: $\Delta U_{SL} = U_{SL} - \sum x_i U_{SL}^i$

Where U_{SL} is the total static energy per formula unit of a specific compound. x_i with i = Li_2O, B_2O_3, and LiCl represents the compositional ratio of each reference phase for which the total static energy per formula unit is denoted by U_{SL}^i.

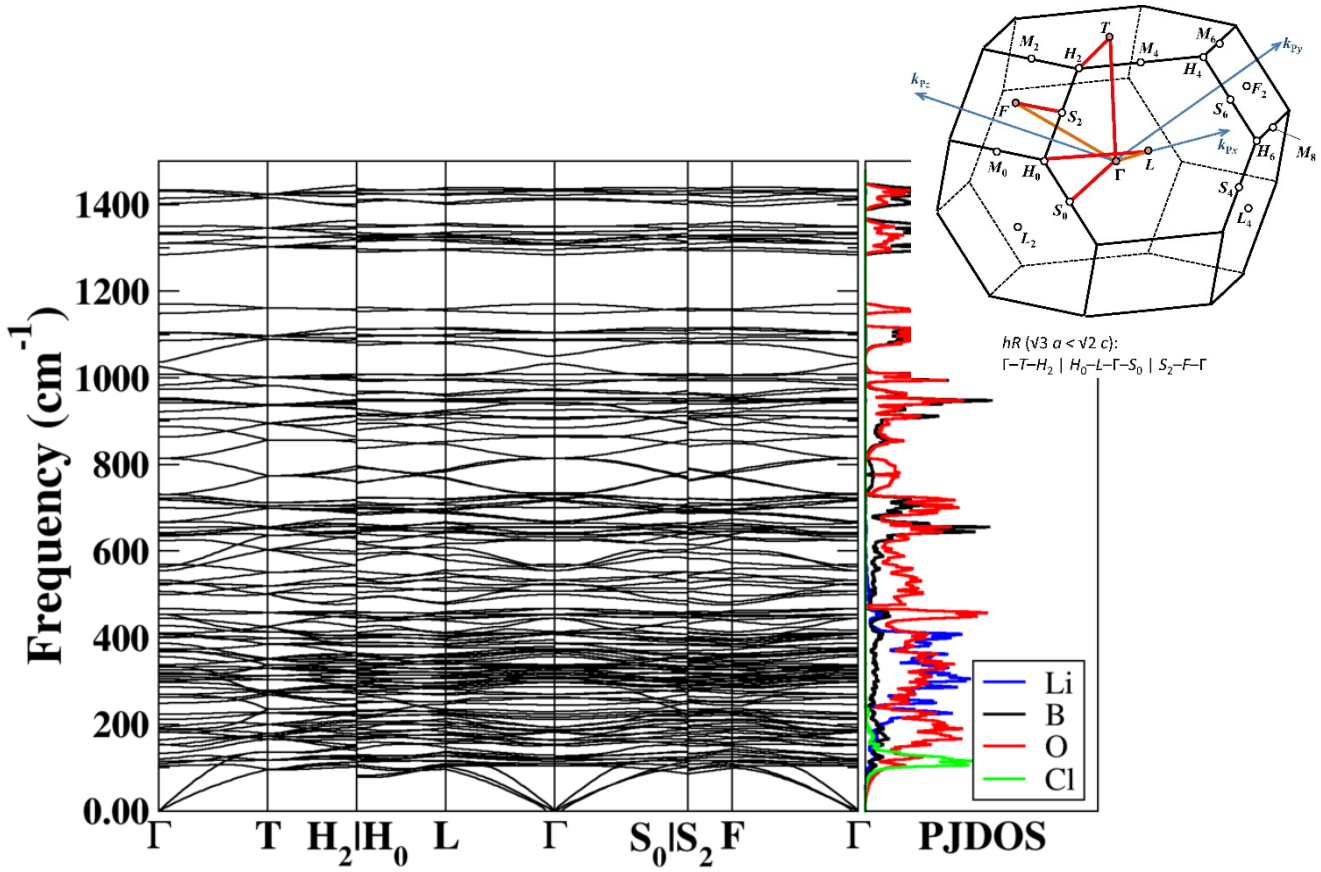

Phonon dispersion curves and projected density states of $Li_4B_7O_{12}Cl$ with frequencies ranging from 0 ~ 1440 cm^{-1}.

Brillouin zone diagram: Hinuma et al., *Comp. Mat. Sci.* **128**, 140-184 (2017). Note that the rhombohedral lattice is described by an equivalent hexagonal system.

NEB analysis for α-$Li_4B_7O_{12}Cl$

$E_{hb} < E_{ha} < E_{mb}$

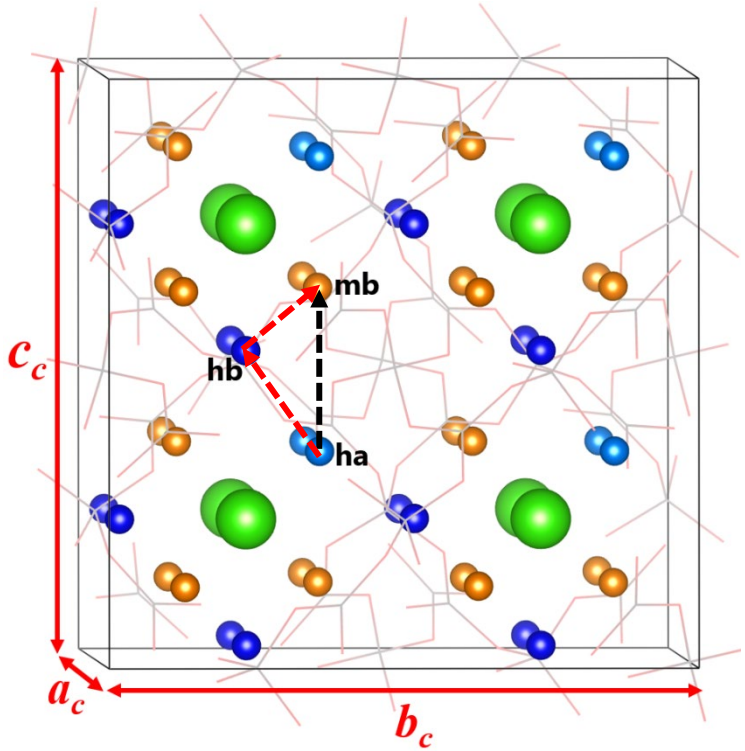

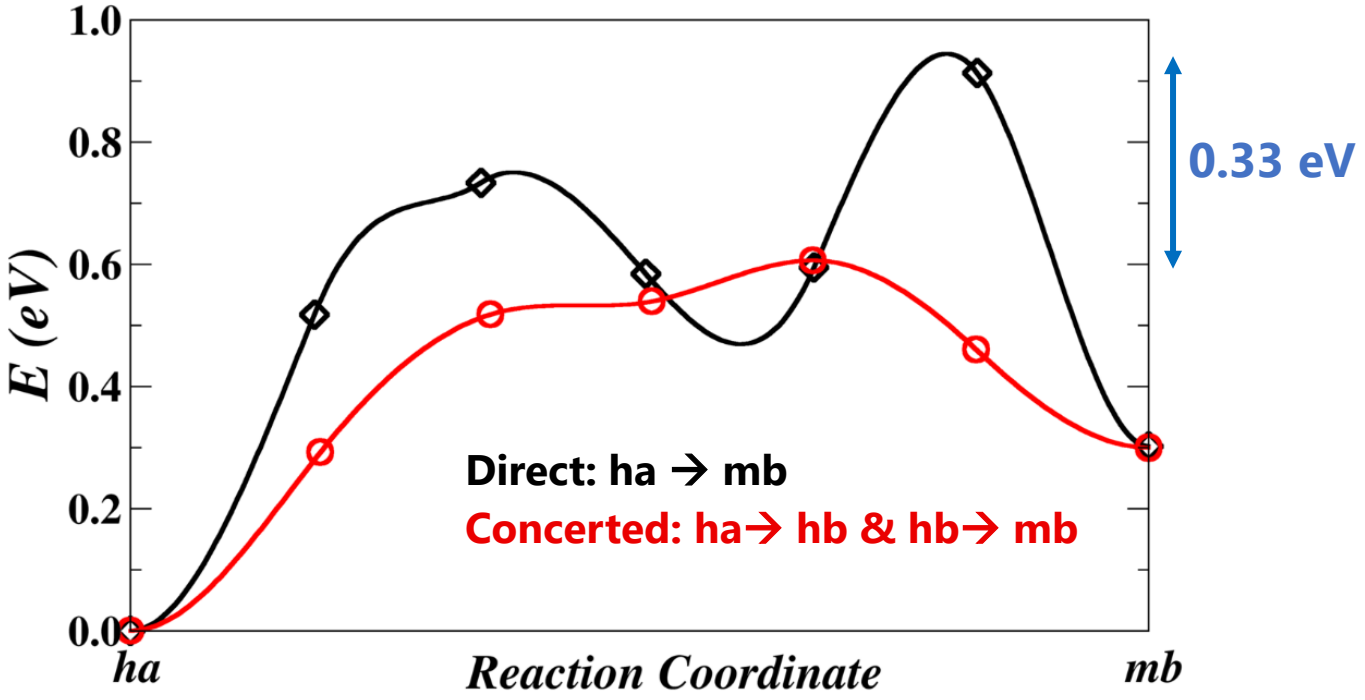

hb: host b-type site; **ha:** host a-type site

mb: metastable b-type site (native vacancy)

→ The concerted migration mechanism reduces the energy barrier for Li ion conduction in α-$Li_4B_7O_{12}Cl$.

NEB: [1]Jónsson et al., *in Classical and Quantum Dynamics in Condensed Phase Simulations*, World Scientific, Singapore (1998)
[2]Henkelman et al., *J. Chem. Phys.* **113**, 9901-9904 (2000)

Results of molecular dynamic simulations

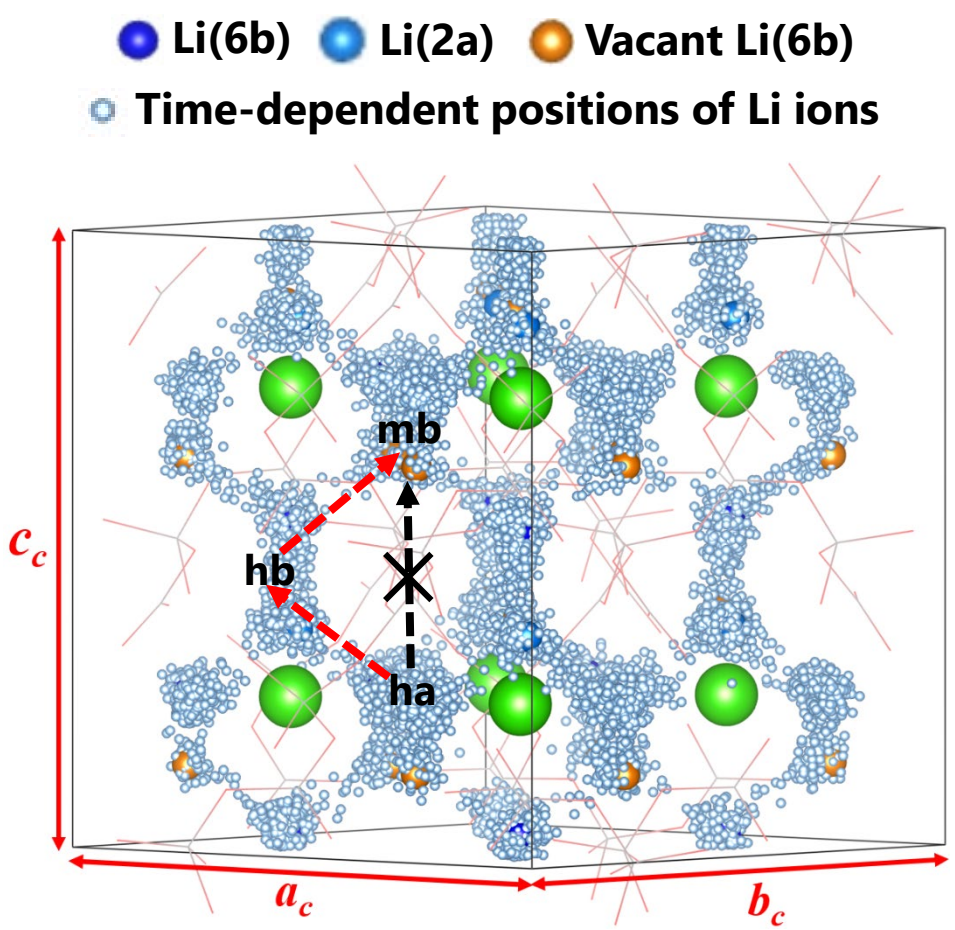

Model of $Li_4B_7O_{12}Cl$ crystal cell with superposed Li positions of molecular dynamics simulation at <T> = 1162 K.

Site occupancy factor: $f_s(\mathrm{t}) = \frac{1}{N_s^{Li}} \sum_{i=1}^{N^{\mathrm{Li}}} n_s^i(t), i = 1, 2, \ldots, N^{\mathrm{Li}}$

Time-averaged: $\bar{f}_s(\mathrm{t}) = \frac{1}{t} \int_0^t f_s(t')dt'$

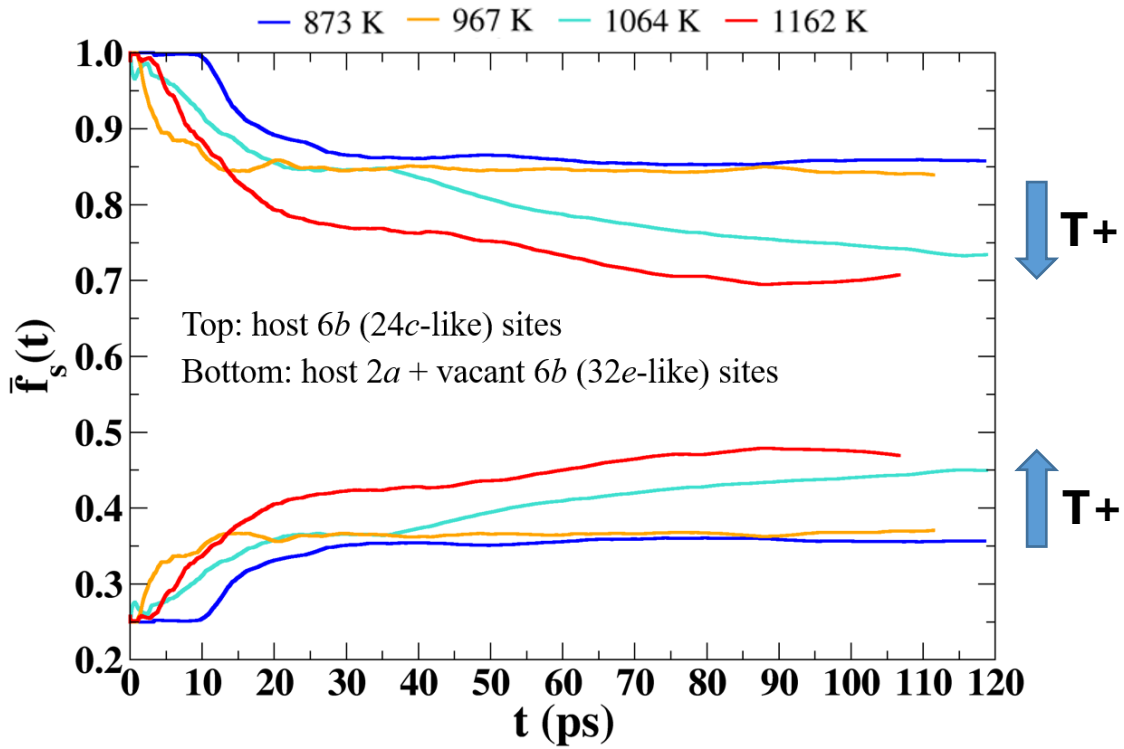

*Recall: the three reported forms **α (T< 310 K), β (310 K <T < 348 K), γ (T > 348 K)** mainly differ in lattice site occupancy.

Ionic conductivities

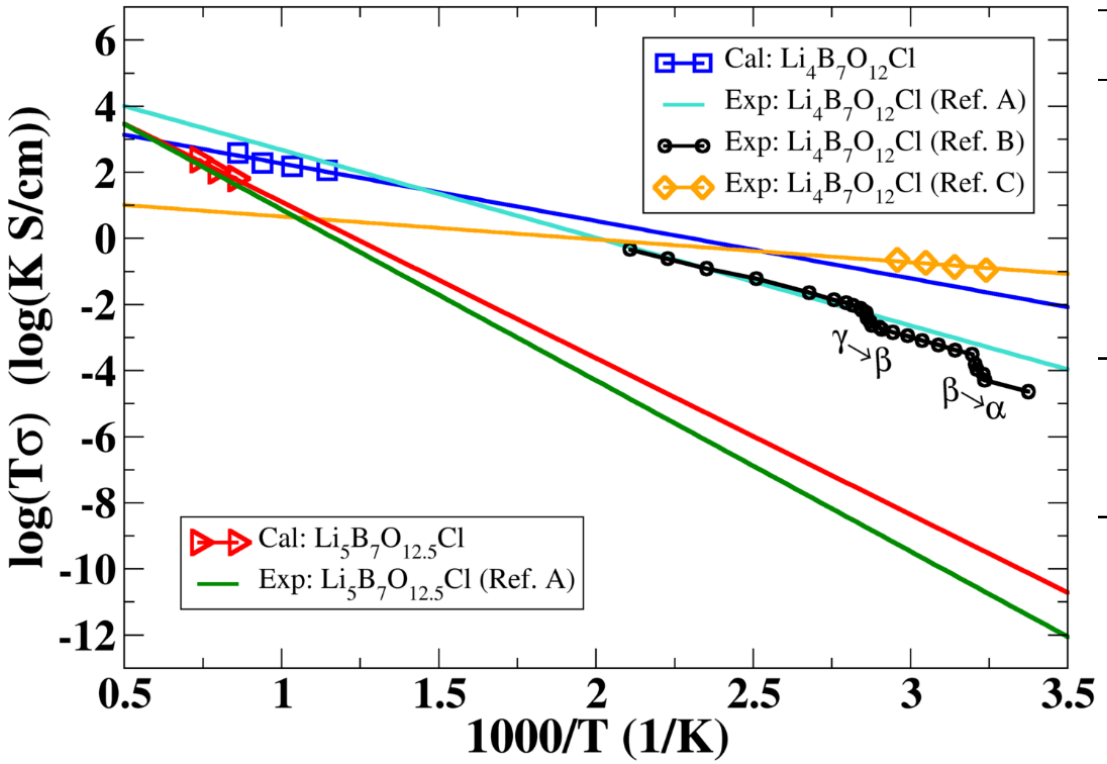

Materials	Analysis	Samples	E_a (eV)	σ (T = 300 K, S/cm)
$Li_4B_7O_{12}Cl$	Cal.	Ideal	0.34	3.83×10^{-4}
	Exp: Ref (A)	Polycrystalline	0.53	1.00×10^{-7}
	Exp: Ref (B)	Single crystal	0.49	0.98×10^{-7}
	Exp: Ref (C)	Polycrystalline	0.14	3.68×10^{-4}
$Li_5B_7O_{12.5}Cl$*	Cal.	Ideal	0.84	6.58×10^{-12}
	Exp: Ref (A)	Polycrystalline	1.03	2.14×10^{-14}

$$\sigma(T) = \rho q^2 \frac{D_{tr}(T)}{k_B T H_r} \quad \text{with} \quad H_r = 1,\ D_{tr}(T) = D_0 e^{-E_a^{\mathrm{MD}}/k_B T}$$

*The ordered $Li_5B_7O_{12.5}Cl$ has a similar B-O framework with $Li_4B_7O_{12}Cl$ but a different ordering of Li ions.

Ref. A: Cales *et al., Solid State Commun.* **24**, 323 (1977)
Ref. B: Jeitschko *et al., Acta Cryst.* B. **33**, 2767-2775 (1977)
Ref. C: Tan *et al., ACS Appl. Energy Mater.* **2**, 5140 (2019).

Ionic substitutions in α-$Li_4B_7O_{12}Cl$

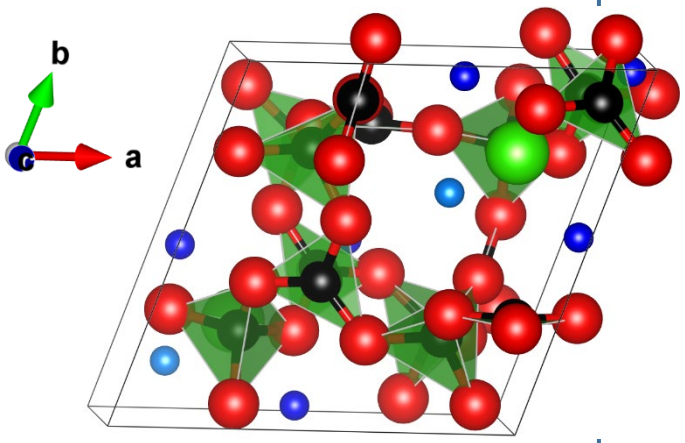

$Li_4B_7O_{12}Cl$

Original material

Rhombohedral R3c

$a_p = b_p = c_p = 8.574$ Å

$\alpha_p = \beta_p = \gamma_p = 60.124°$

$a_c = b_c = c_c = 12.137$ Å

$\alpha_c = \beta_c = \gamma_c = 90.108°$

B(1) → Al

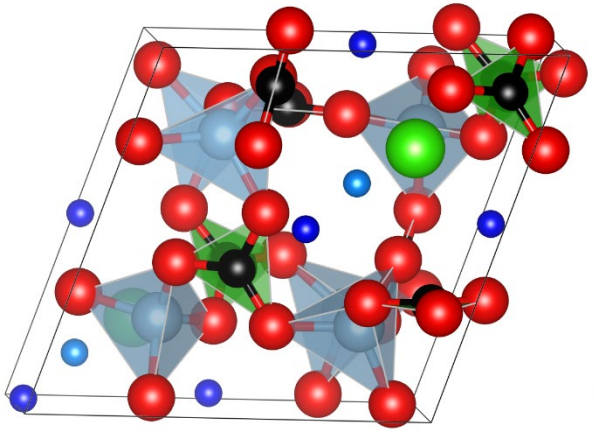

$Li_4Al_3B_4O_{12}Cl$

Realized in experiment*

Rhombohedral R3c

$a_p = b_p = c_p = 9.133$ Å

$\alpha_p = \beta_p = \gamma_p = 61.194°$

$a_c = b_c = c_c = 13.033$ Å

$\alpha_c = \beta_c = \gamma_c = 91.022°$

*Kajihara *et al.*, *Bull. Chem. Soc. Jpn.* **90**, 1279–1286 (2017)

O → S

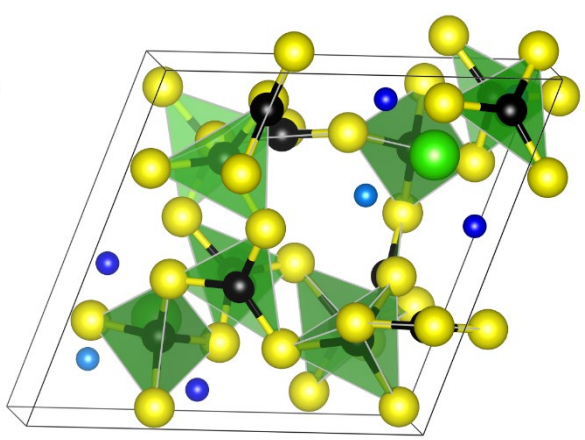

$Li_4B_7S_{12}Cl$

Predicted in this work

Rhombohedral R3c

$a_p = b_p = c_p = 10.584$ Å

$\alpha_p = \beta_p = \gamma_p = 59.704°$

$a_c = b_c = c_c = 14.934$ Å

$\alpha_c = \beta_c = \gamma_c = 89.743°$

B(1) → Al & O → S

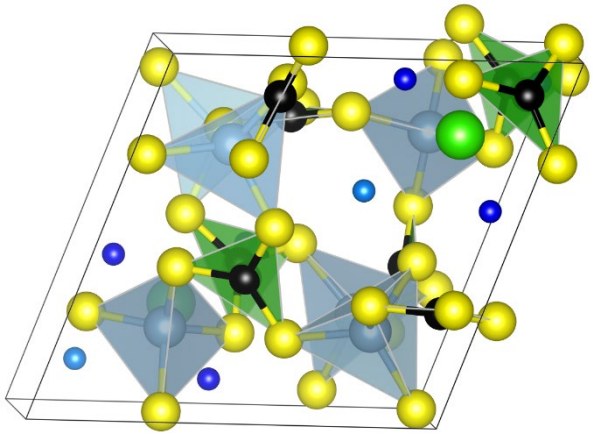

$Li_4Al_3B_4S_{12}Cl$

Predicted in this work

Rhombohedral R3c

$a_p = b_p = c_p = 11.386$ Å

$\alpha_p = \beta_p = \gamma_p = 68.601°$

$a_c = b_c = c_c = 15.933$ Å

$\alpha_c = \beta_c = \gamma_c = 88.771°$

Comparison of diffusional properties

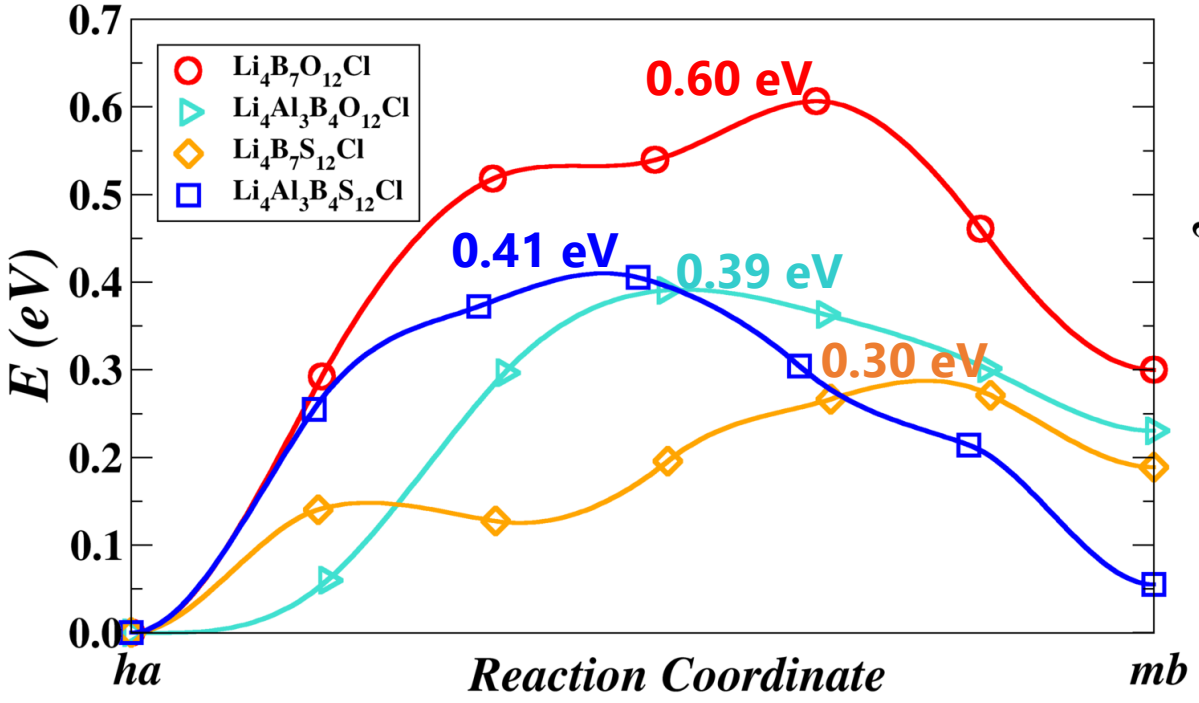

NEB energy diagram of concerted migrations

MD for S analog (Cory Lynch)

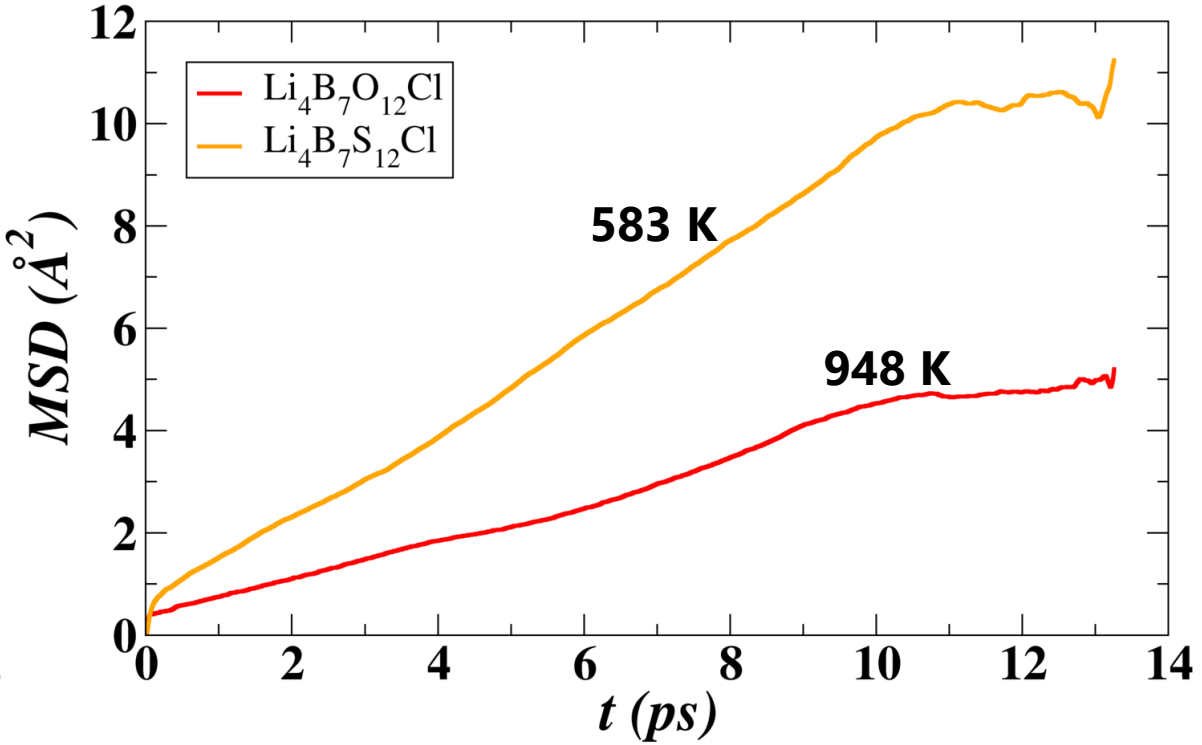

Mean squared displacement vs. time interval

Are the analog compounds stable?

$Li_4Al_3B_4O_{12}Cl$ Kajihara *et al.*, *Bull. Chem. Soc. Jpn.* **90**, 1279–1286 (2017)

$$Li_4Al_3B_4O_{12}Cl \rightarrow 1/2\ Li_4B_7O_{12}Cl + 1/2\ LiB + 1/2\ LiClO_4 + LiAlO_2 + 2\ AlO - 14.29\ eV$$

$$Li_4Al_3B_4O_{12}Cl \rightarrow 1/2\ Li_4B_7O_{12}Cl + 1/2\ Al_5BO_9 + 1/2\ AlClO + Li_2O - 0.8\ eV$$

$Li_4B_7S_{12}Cl$ (proposed)

$$Li_4B_7S_{12}Cl \rightarrow 3\ Li + 7\ B + 12\ S + LiCl - 14.38\ eV$$

$$Li_4B_7S_{12}Cl \rightarrow Li_3BS_3 + 3\ B_2S_3 + LiCl + 0.46\ eV$$

$Li_4Al_3B_4S_{12}Cl$ (proposed)

$$Li_4Al_3B_4S_{12}Cl \rightarrow 3\ Li + 3\ Al + 4\ B + 12\ S + LiCl - 18.35\ eV$$

$$Li_4Al_3B_4S_{12}Cl \rightarrow 3/2\ Li_2S + 3/2\ Al_2S_3 + 2\ B_2S_3 + LiCl + 0.87\ eV$$

Phonon calculations

Predicted

$Li_4B_7S_{12}Cl$

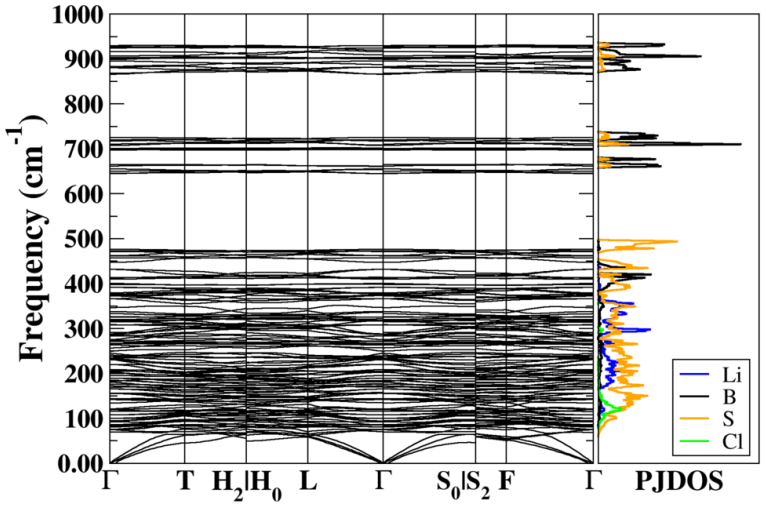

0 cm^{-1} ≤ ω(q) ≤ 931 cm^{-1}

Known

$Li_4B_7O_{12}Cl$

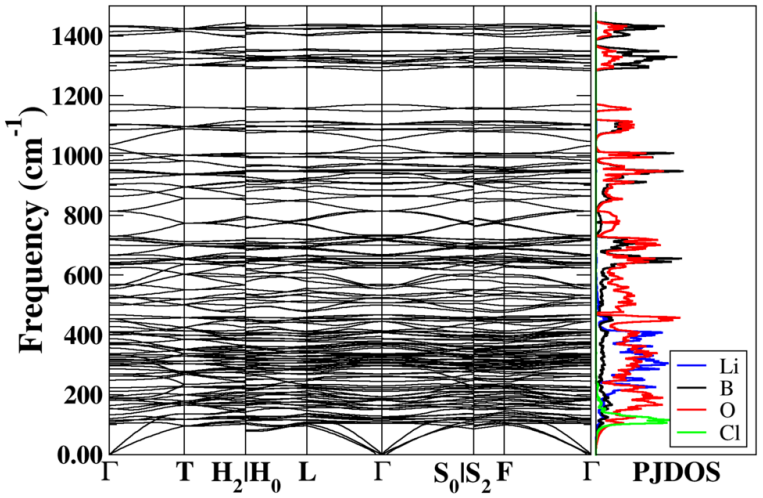

0 cm^{-1} ≤ ω(q) ≤ 1440 cm^{-1}

$$F_{vib}(T) = k_B T \int_0^\infty d\omega \ln\left(2\sinh\left(\frac{\hbar\omega}{2k_B T}\right)\right) g(\omega)$$

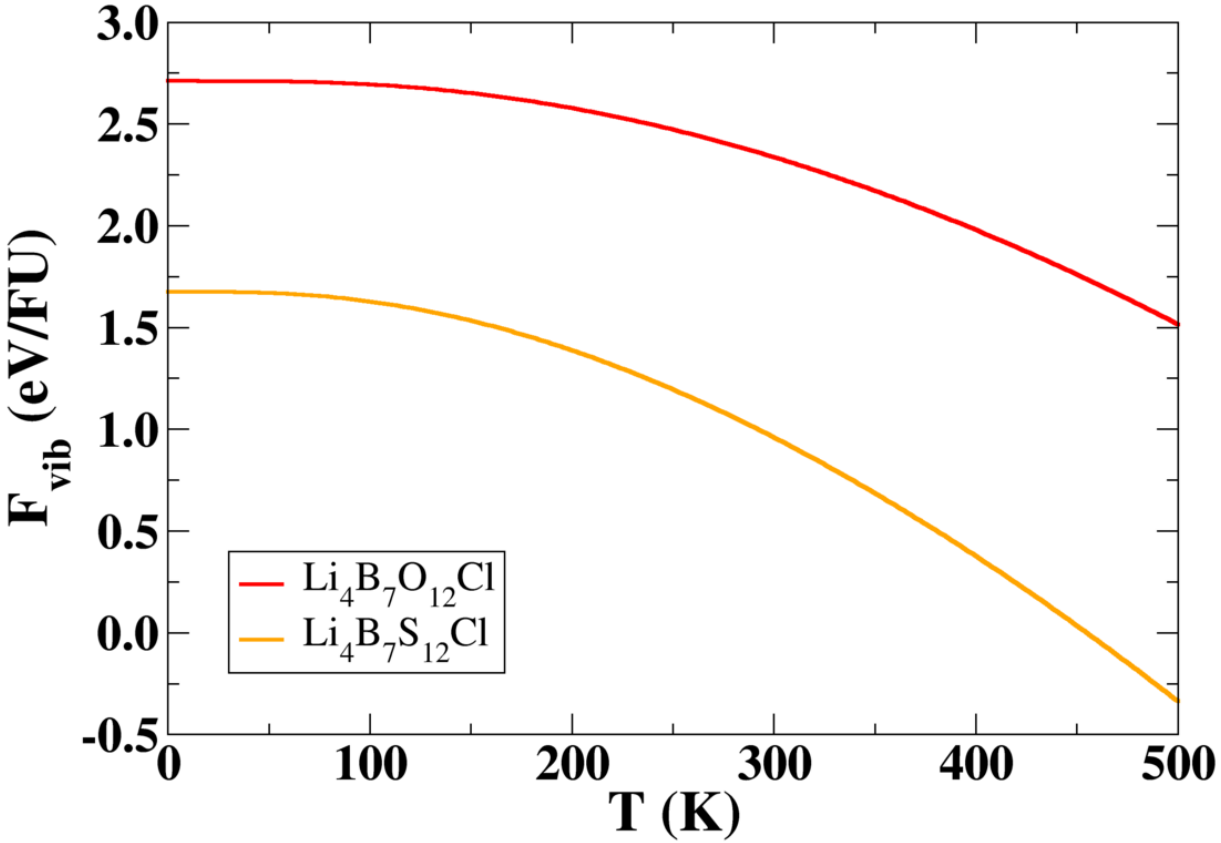

ΔF_{vib} (T = 300 K) = 1.38 eV/FU

Summary of the project

- The ground state structure of the room-temperature form of $Li_4B_7O_{12}Cl$ is identified to have rhombohedral R3c symmetry. The phase is estimated to be stable from the analysis of the convex hull approach and of the phonon spectrum.
- The NEB calculations indicate that Li ion migration in $Li_4B_7O_{12}Cl$ most likely proceeds via concerted migration mechanisms involving two host sites and one natural vacancy.
- The room-temperature ionic conductivity of $Li_4B_7O_{12}Cl$, calculated from the MD simulation results, is on the order of 10^{-4} S/cm, which is in good agreement with the recent experimental measurement for pure polycrystalline samples.
- Consistent with the recent experimental results, our preliminary calculations also find reduced Li ion migration barriers in the partially B-replaced compound $Li_4Al_3B_4O_{12}Cl$. The studies on predicted compounds $Li_4B_7S_{12}Cl$ and $Li_4Al_3B_4S_{12}Cl$ also suggest improved Li ion conducting performance compared with $Li_4B_7O_{12}Cl$.
- The chemical stabilities of the $Li_4B_7S_{12}Cl$ and $Li_4Al_3B_4S_{12}Cl$ need further investigation.

Manuscript to be submitted

Outline

- Research background: General motivation and theoretical tools
- **Finished/ongoing projects: Inputs and outcomes**

$Na_4P_2S_6$, $Li_4P_2S_6$, and possible alloy

Yan Li, Zachary D. Hood, and N. A. W. Holzwarth

Phys. Rev. Mater. 4, 045406 (2020)

Phonon dispersion

Yan Li, W. C. Kerr, and N. A. W. Holzwarth

J. Condens. Matter Phys. 32, 055402 (2020)

Li_3BO_3 and Li_3BN_2 (I & II)

Yan Li, Zachary D. Hood, and N. A. W. Holzwarth

Phys. Rev. Mater. 5, 085402 & 085403 (2021)

$Li_{4+x}B_7O_{12+x/2}Cl$ (x = 0, 1) and related

$Li_{7.5}B_{10}S_{18}X_{1.5}$ (X = Cl, Br, I)

New fast Li ion electrolytes $Li_{7.5}B_{10}S_{18}X_{1.5}$

$Li_{7.5}B_{10}S_{18}X_{1.5}$ (X = Cl, Br, I)

Monoclinic C2/c (No. 15)

Disordered Li and X sites

Room-T σ ~ mS/cm

GDCh Communications Angewandte International Edition

VIP Ion Conductivity Very Important Paper

How to cite: *Angew. Chem. Int. Ed.* **2021**, *60*, 6975–6980
International Edition: doi.org/10.1002/anie.202013339
German Edition: doi.org/10.1002/ange.202013339

Fast Li-Ion Conductivity in Superadamantanoid Lithium Thioborate Halides

*Kavish Kaup, Abdeljalil Assoud, Jue Liu, and Linda F. Nazar**

[*] K. Kaup, A. Assoud, L. F. Nazar
Department of Chemistry, Department of Chemical Engineering and the Waterloo Institute for Nanotechnology, University of Waterloo
200 University Ave W, Waterloo, Ontario N2L 3G1 (Canada)
E-mail: lfnazar@uwaterloo.ca

J. Liu
Neutron Scattering Division, Oak Ridge National Laboratory
Oak Ridge, TN 37831 (USA)

lithium and halide anion disorder. The phases are non-stoichiometric, adopting slightly varying halide contents within the materials. These new superadamantanoid materials exhibit high ionic conductivities up to 1.4 mS cm^{-1}, which can be effectively tuned by the polarizability of the halide anion within the channels.

of supertetrahedral clusters (also antanoid) $B_{10}S_{20}$ structural units. ructures were observed in lithium licates,[11,12] lithium nitridophos- er thioborates such as $Ag_6B_{10}S_{18}$ any other sulfide-based materi- etworks are of interest because the l anions to distribute into the void . For frameworks with a large void akly bonded to the surrounding tion mobility within the structure. For such materials, the highest reported room-temperature ionic conductivity is only 4×10^{-4} S cm^{-1} for sodium phosphidosilicates,[11] and $\approx 10^{-7}$ S cm^{-1} for lithium phosphidosilicates.[21] An ionic conductivity greater than 10^{-4} S cm^{-1} is often considered fast, but at least 10^{-3} S cm^{-1} is necessary to achieve practical solid-state batteries.[22]

Kaup *et al.* 2021

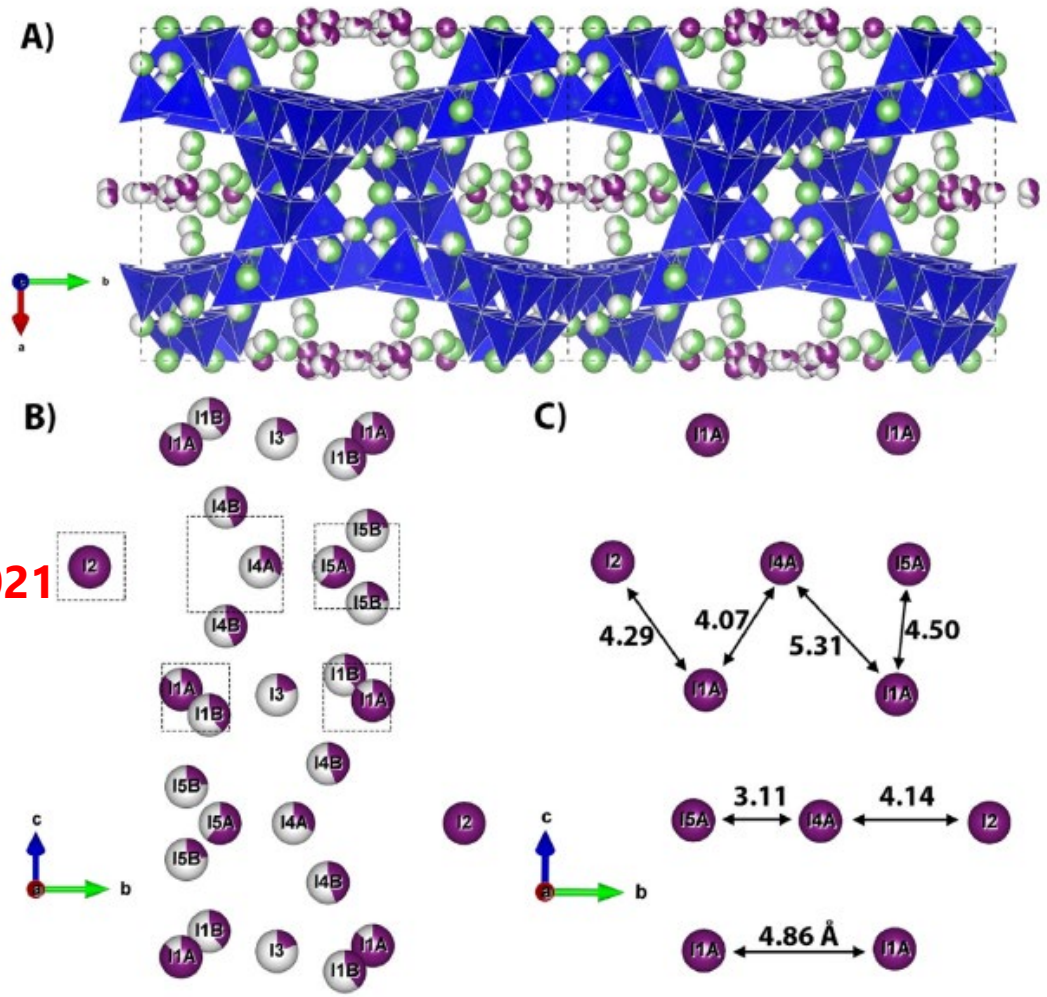

Figure 3. A) $Li_{7.5}B_{10}S_{18}I_{1.5}$ structure with lithium and iodine in the channels. B) Average structure (refined from NPD at 300 K) and C) local structure (refined from NPDF at 290 K) of iodine in the tunnels. The iodide ions distributed through the channel are positioned in groups, as indicated by the dashed boxes in (B).

Comparison of the current and previous projects

Similarities –

- Same atomic elements
- B-S framework + large voids for Li and Cl
- Favorable Li ion conductivity

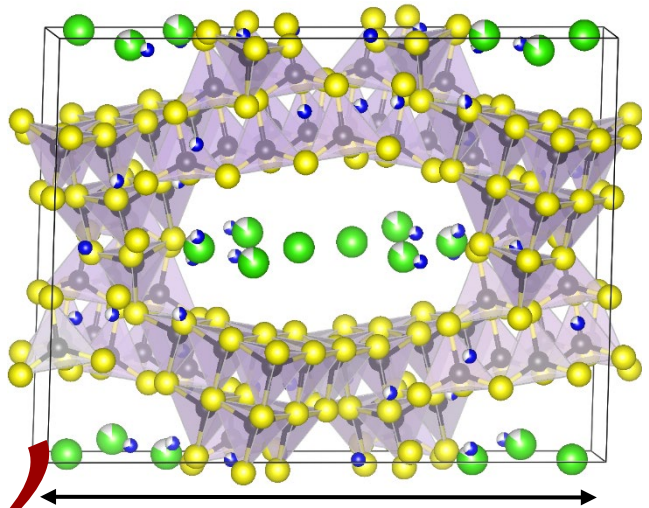

b = 21.2 Å > *a* > *c*

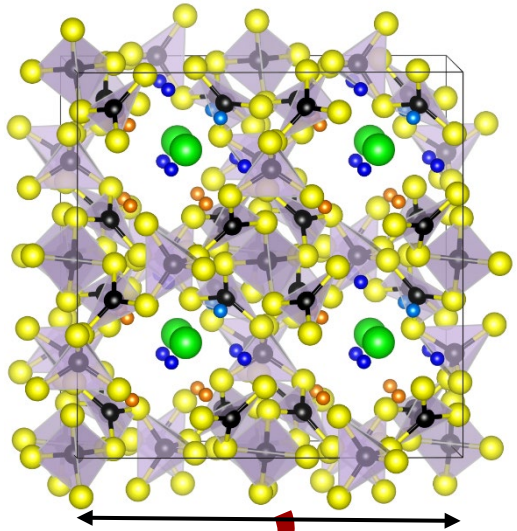

a = b = c = 14.9 Å

Differences –

$Li_{7.5}B_{10}S_{18}Cl_{1.5}$

- Experimentally realized; chemically stable
- Framework based on BS_4 tetrahedra
- Low symmetry structure (monoclinic)
- Large voids without obvious structure
- 148 ions in MD simulation cell (primitive C2/c lattice)

$Li_4B_7S_{12}Cl$

- Not (yet) experimentally realized; chemical reactivity
- Framework based on BS_4 + BS_3 units
- Based on ordered rhombohedral structure
- Structured voids
- 196 ions in MD simulation cell (similar to conventional FCC lattice)

Structure of $Li_{7.5}B_{10}S_{18}Cl_{1.5}$

From experiment

$Li_{7.5}B_{10}S_{18}Cl_{1.5}$ from Kaup *et al.* (2021)

Monoclinic C2/c (No. 15)

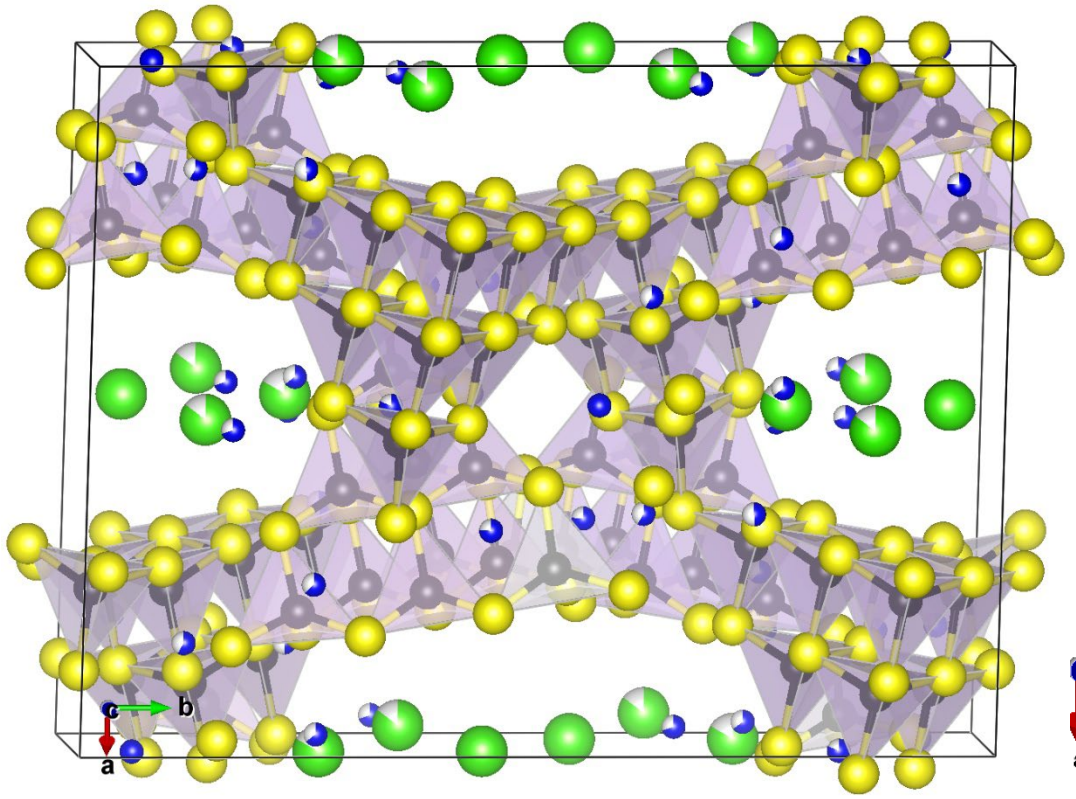

Some Li ions are missing

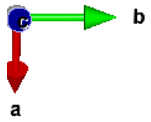

From computation

$Li_{7.5}B_{10}S_{18}Cl_{1.5}$ from DFT optimization

Monoclinic C2/c (No. 15)

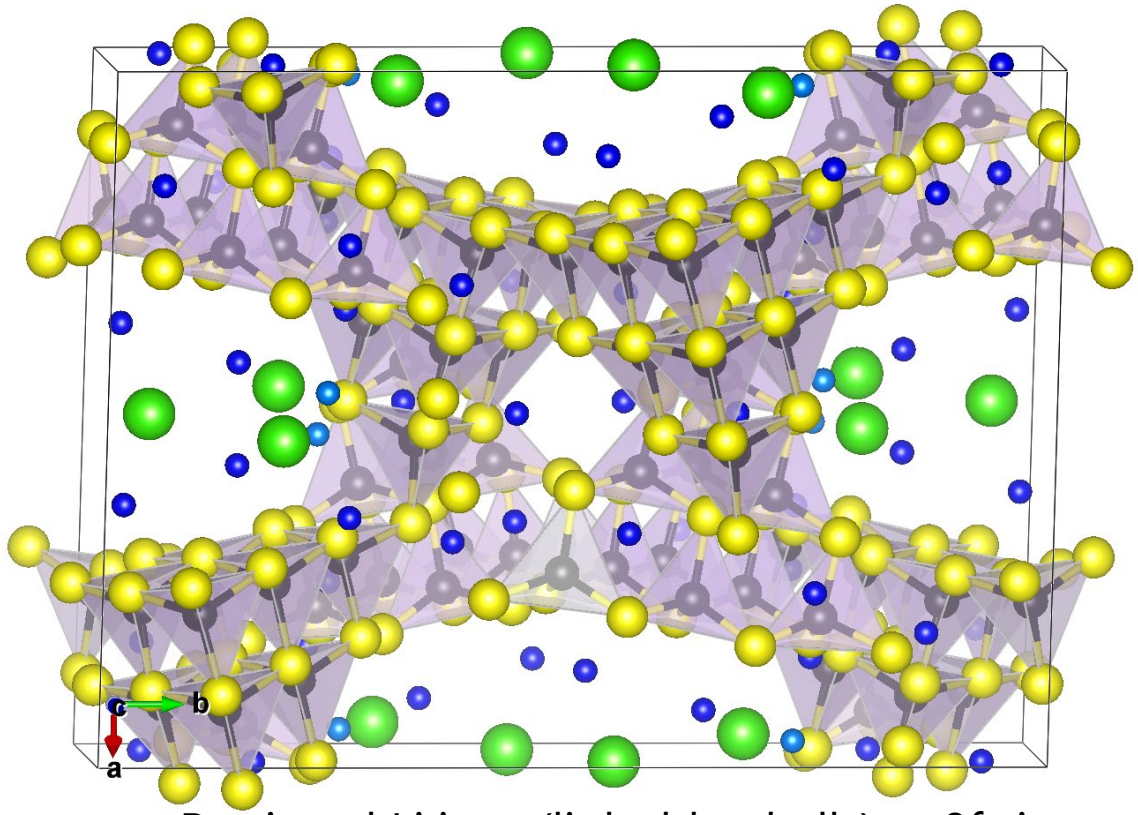

Retrieved Li ions (light blue balls) at 8f site

Optimized vs. experimental structures

$Li_{7.5}B_{10}S_{18}Cl_{1.5}$ $Li_{7.5}B_{10}S_{18}Br_{1.5}$ $Li_{7.5}B_{10}S_{18}I_{1.5}$

From calc ➔ DFT opt (at 0 K)

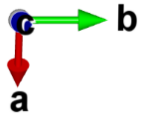

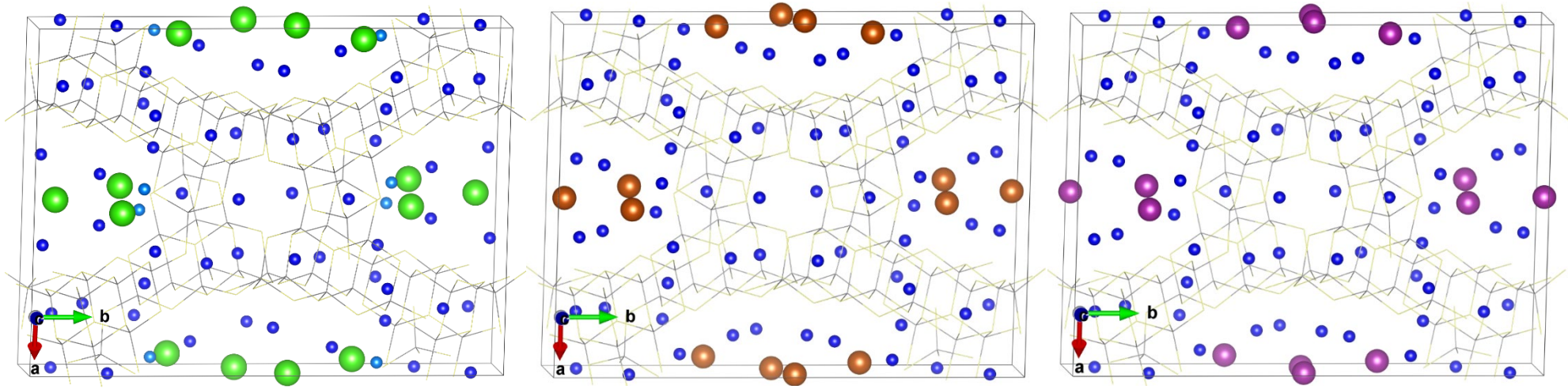

From exp ➔ (at 300 K)

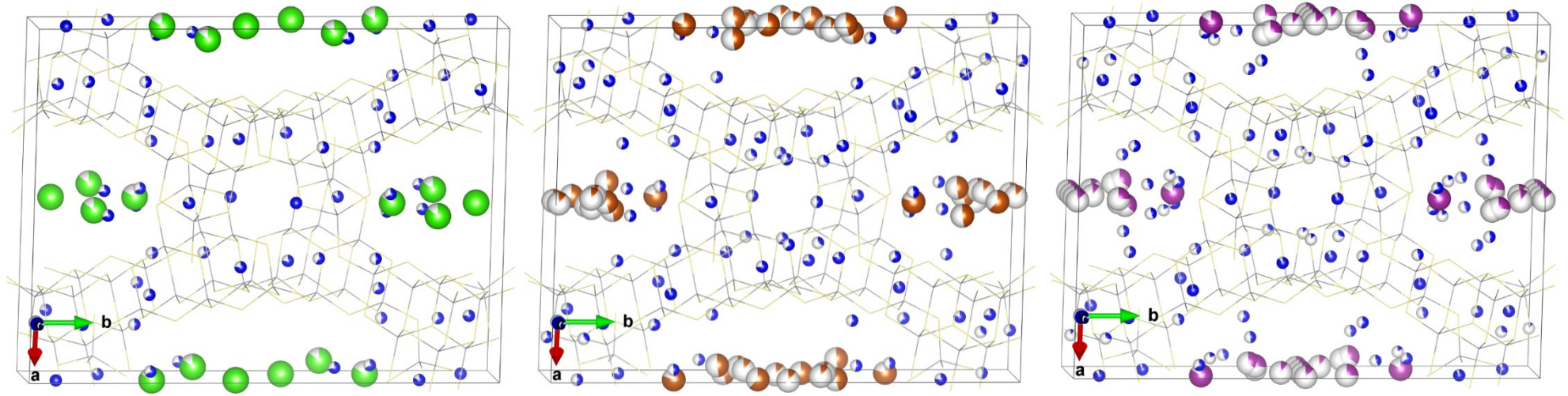

Comparison of lattice parameters

Numerical comparison of conventional lattice parameters of optimized ("cal") and experimental (Kaup *et al.*)) $Li_{7.5}B_{10}S_{18}X_{1.5}$ (X=Cl, Br, I).

	X = Cl (cal. /exp.)	X = Br (cal. /exp.)	X = I (cal. /exp.)
a (Å)	20.96/21.16	20.88/21.21	21.09/21.32
b (Å)	21.66/22.23	21.19/21.25	21.40/21.27
c (Å)	16.02/16.13	16.07/16.26	16.08/16.21
α = γ (deg)	90.00/90.00	90.00/90.00	90.00/90.00
B (deg)	128.75/128.92	128.43/128.82	128.70/128.77
Volume (Å^3)	5672.62/5638.31	5572.37/5708.07	5664.13/5731.36

Pair distribution analysis: From neutron scattering (Kaup *et al.*)

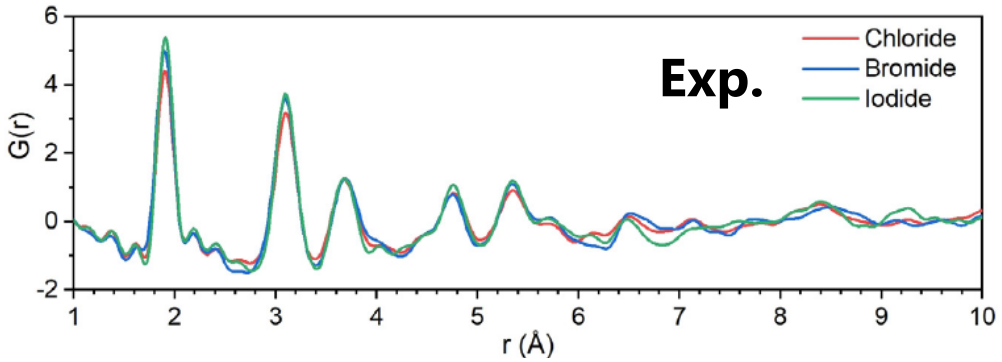

From molecular dynamics simulations (This work at 400 K over 30 ps)

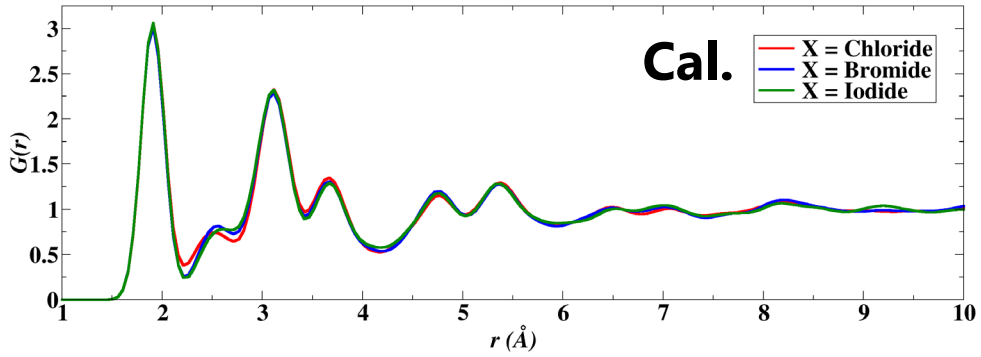

Computational estimate of chemical stability

Based on DFT static lattice calculations, several decomposition pathways indicate endothermic reactions at equilibrium and suggest chemical stability of $Li_{7.5}B_{10}S_{18}X_{1.5}$

$$Li_{7.5}B_{10}S_{18}Cl_{1.5} \rightarrow 1.5\ LiCl + 5\ B_2S_3 + 3\ Li_2S - 0.8\ eV$$

$$Li_{7.5}B_{10}S_{18}Cl_{1.5} \rightarrow 1.5\ LiCl + 4\ B_2S_3 + 2\ Li_3BS_3 - 1.0\ eV$$

$$Li_{7.5}B_{10}S_{18}Br_{1.5} \rightarrow 1.5\ LiBr + 5\ B_2S_3 + 3\ Li_2S - 0.9\ eV$$

$$Li_{7.5}B_{10}S_{18}Br_{1.5} \rightarrow 1.5\ LiBr + 4\ B_2S_3 + 2\ Li_3BS_3 - 1.1\ eV$$

$$Li_{7.5}B_{10}S_{18}I_{1.5} \rightarrow 1.5\ LiI + 5\ B_2S_3 + 3\ Li_2S - 1.0\ eV$$

$$Li_{7.5}B_{10}S_{18}I_{1.5} \rightarrow 1.5\ LiI + 4\ B_2S_3 + 2\ Li_3BS_3 - 1.2\ eV$$

Assessing ion mobility in $Li_{7.5}B_{10}S_{18}X_{1.5}$

Define a probability density* for the mobile ions

$$p^a(\mathbf{r}) = \frac{1}{k_{\max}} \sum_{k=1}^{k_{\max}} \sum_{i \in a}^{N^a} \delta(\mathbf{r} - \mathbf{R}_i^a(t_k))$$

N^a -- Number of ions of type *a* within the simulation cell

$\mathbf{R}_i^a(t_k)$ -- Trajectories of ion *i* at sampling time t_k

$k_{\max}$ -- Number of time steps

In practice, the δ function is approximated as an isotropic Gaussian shape

$$\delta(\mathbf{s}) \approx \frac{1}{\left(2\pi\sigma^2\right)^{3/2}} e^{-s^2/2\sigma^2}$$

with σ chosen as 0.2 Å

*He, Zhu, and Mo, *Nat. Comm.* **8**, 15893 (2017)

Isosurface plots of $P^a(r)$

*Visualized along the c-axis from MD simulations at ~800 K

$p^{Li}(r)$ →

$p^{X}(r)$ →

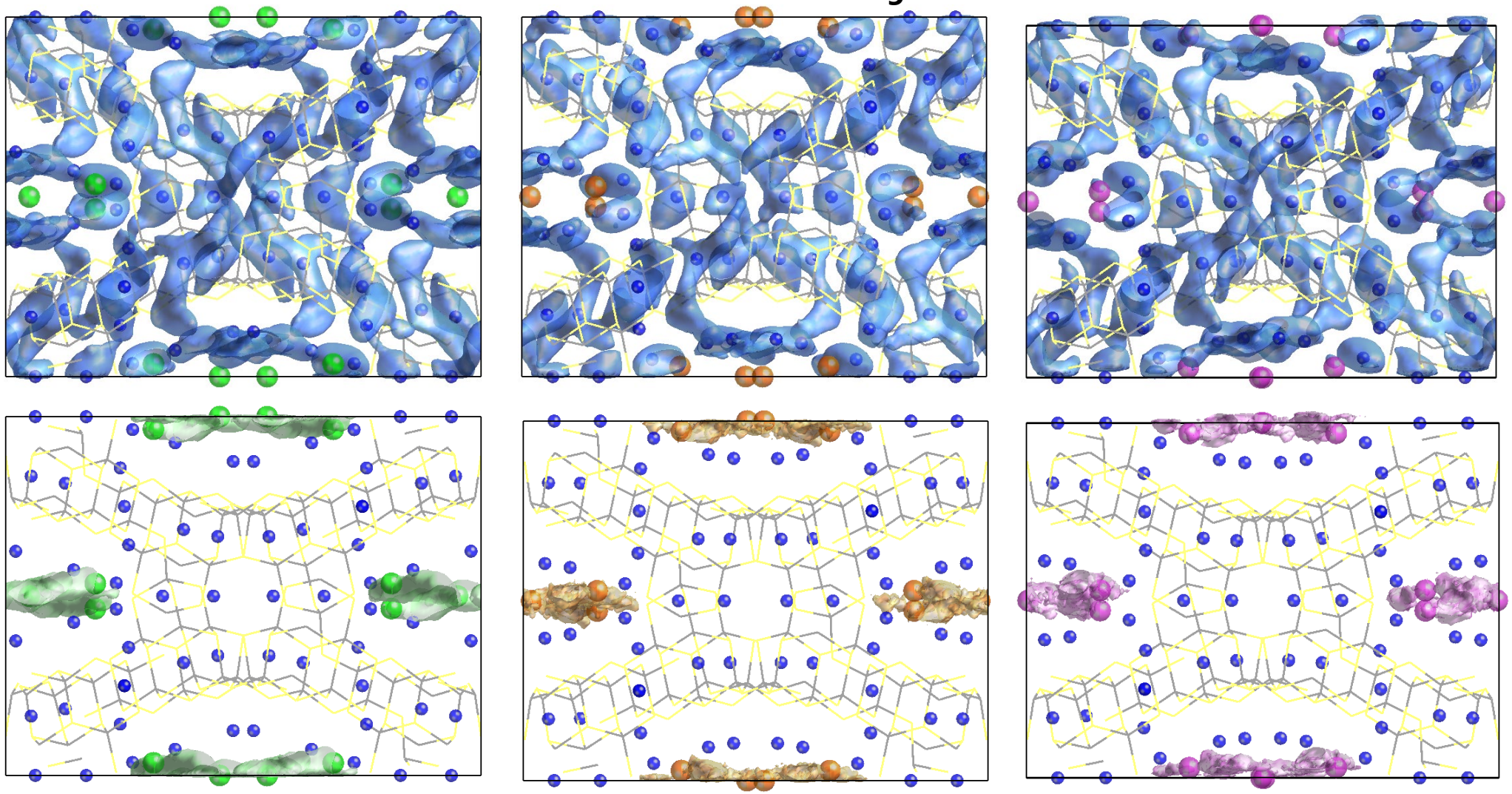

$Li_{7.5}B_{10}S_{18}Cl_{1.5}$ $Li_{7.5}B_{10}S_{18}Br_{1.5}$ $Li_{7.5}B_{10}S_{18}I_{1.5}$

More details on the B-S bonds at T = 800 K

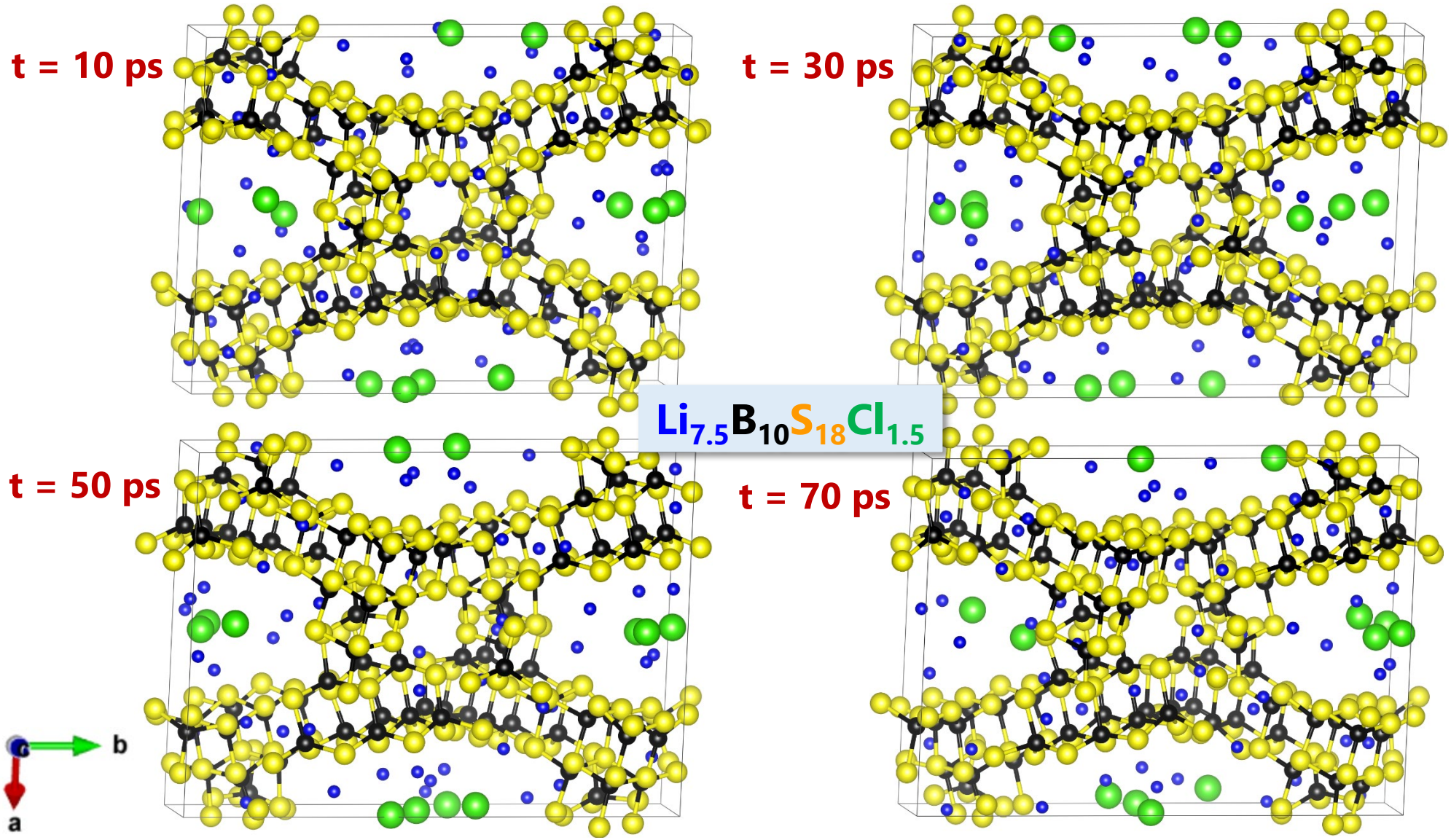

Mean squared displacements of Li ions from MD simulations

For an MD simulation at average temperature T :

$$\mathrm{MSD}(\tau,T)=\frac{1}{N^{\mathrm{Li}}}\left\langle\sum_{i=1}^{N^{\mathrm{Li}}}\left|\mathbf{R}_i^{\mathrm{Li}}(t+\tau)-\mathbf{R}_i^{\mathrm{Li}}(t)\right|^2\right\rangle_t$$

which is related to the tracer diffusion:

$D_{tr}(T)=\lim_{\tau\to\infty}\left(\frac{1}{6\tau}\mathrm{MSD}(\tau,T)\right)$. The Nernst-Einstein relation then leads to an estimate of the ionic conductivity: $\sigma(T)=\frac{N^{\mathrm{Li}}}{V}\frac{e^2D_{tr}(T)}{k_BTH_r}$,

where V = volume, k_B = Boltzmann constant, e = elementary charge, H_r = Haven ratio. It is also reasonable to assume an Arrhenius behavior for the tracer diffusion with activation energy E_a :

$D_{tr}(T)=D_{ref}e^{-E_a/k_BT}$.

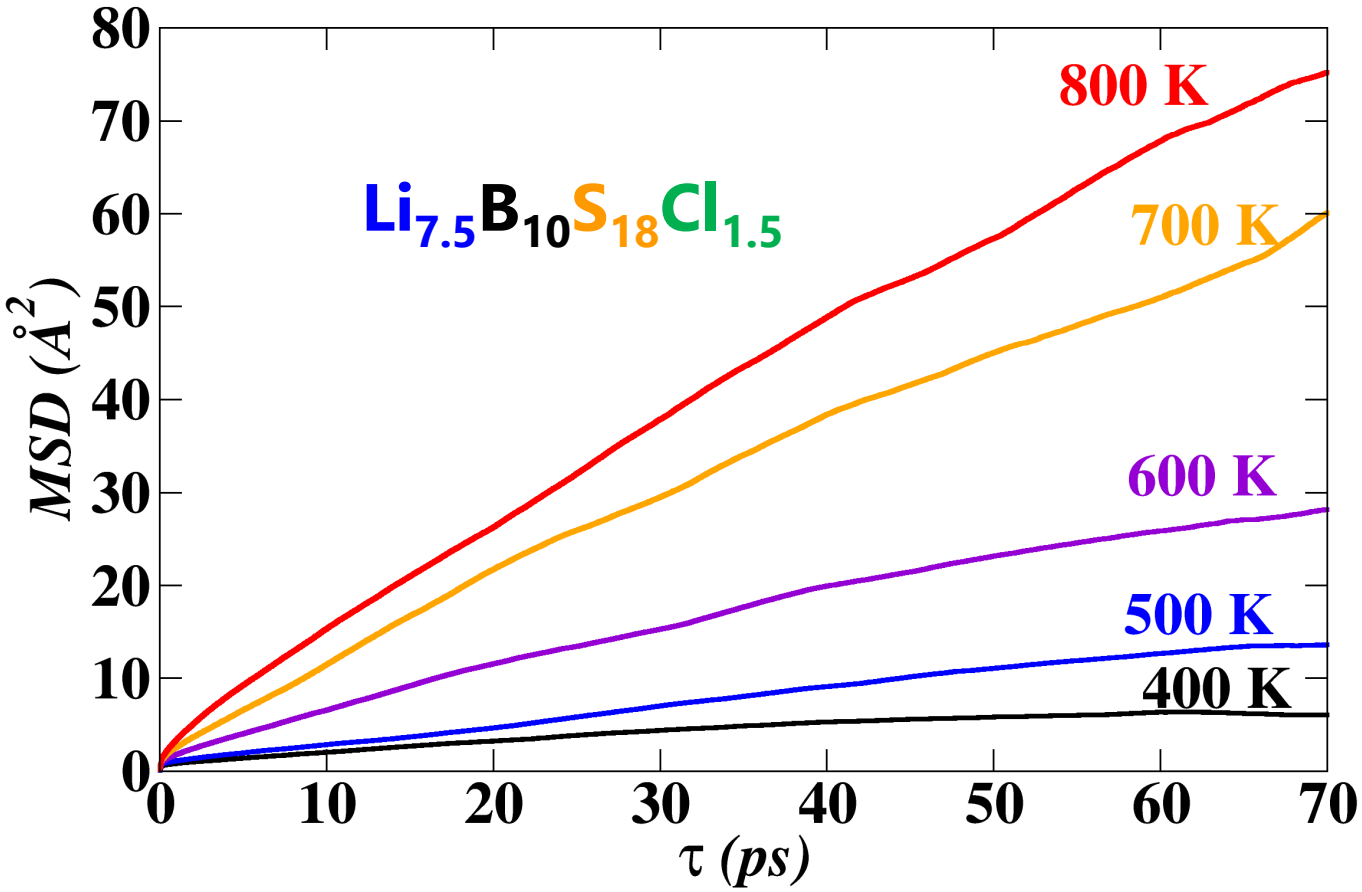

Preliminary MD results for Li ion conductivity

$$\sigma(T) = \frac{N^{\mathrm{Li}}}{V} \frac{e^2 D_{tr}(T)}{k_B T H_r}$$

$$\text{Evaluated for } H_r = \frac{D_{tr}}{D_{tr} + D_{cross}} = 1$$

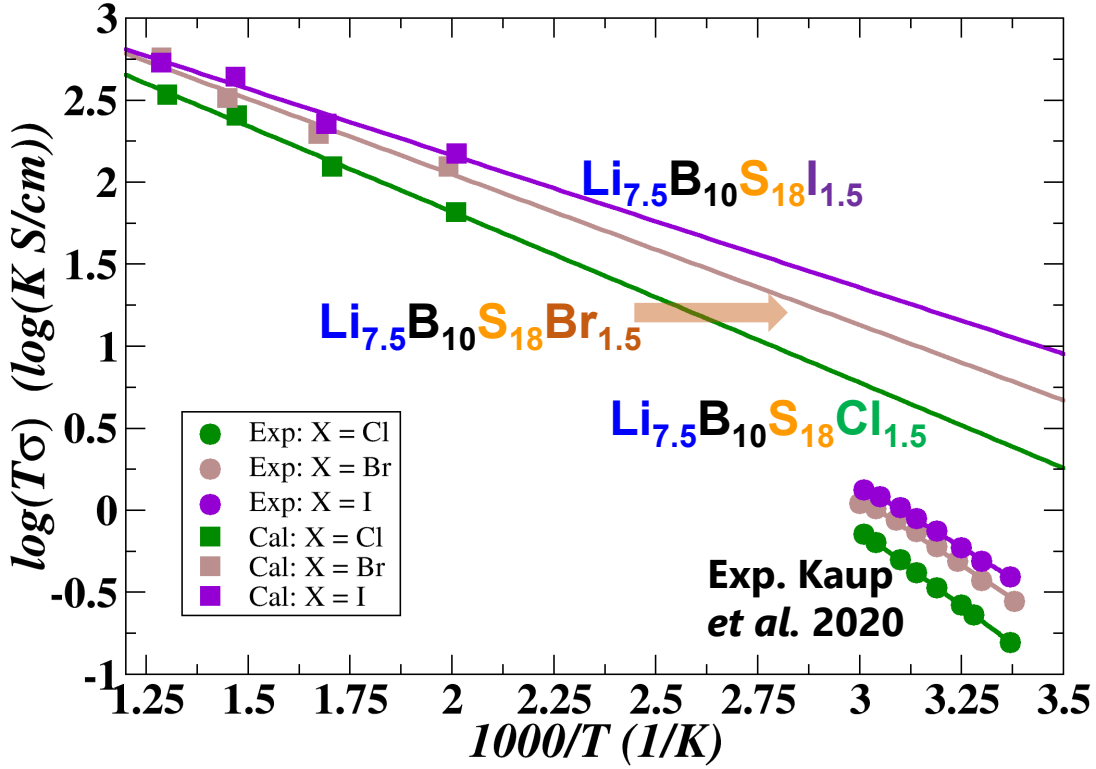

Histogram of numbers of Li ion hops within 100 time intervals of 0.5 ps each at ~800 K

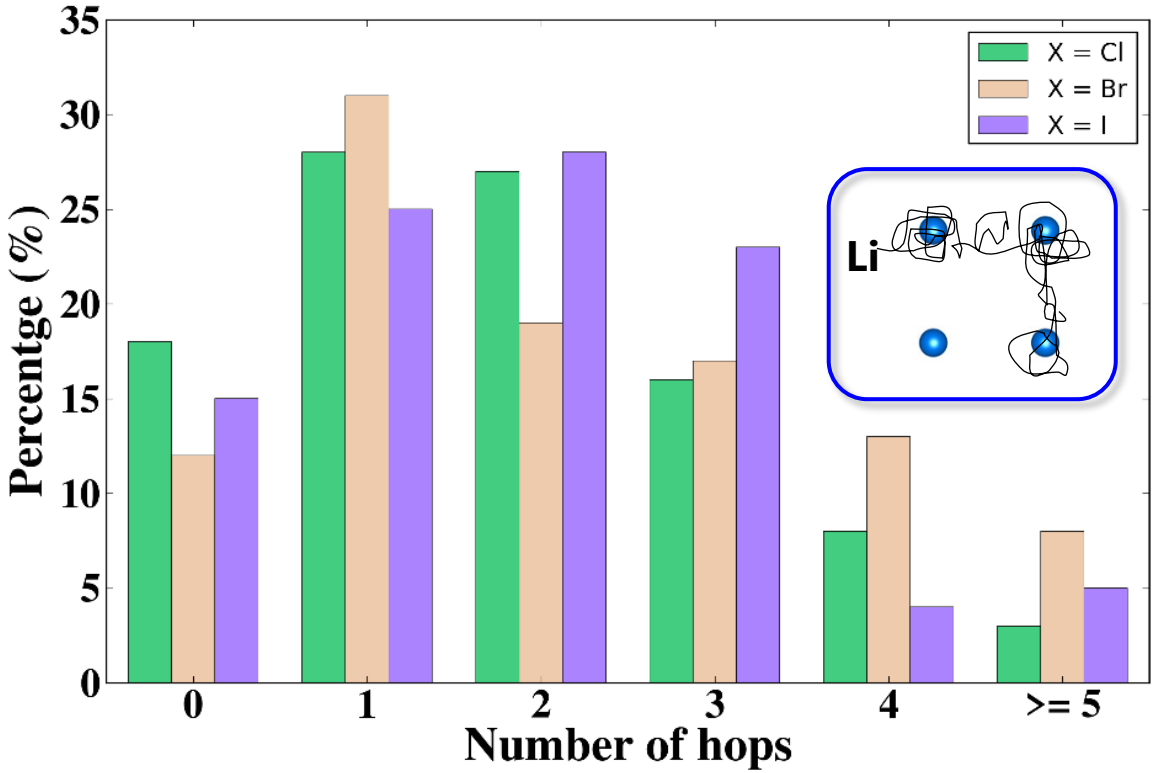

Each hopping event was assessed on the basis of the equilibrium sites of the optimized lattice. A hopping event was tabulated at each arrival time of an ion at a new site.

Further assessment of Li ion correlations

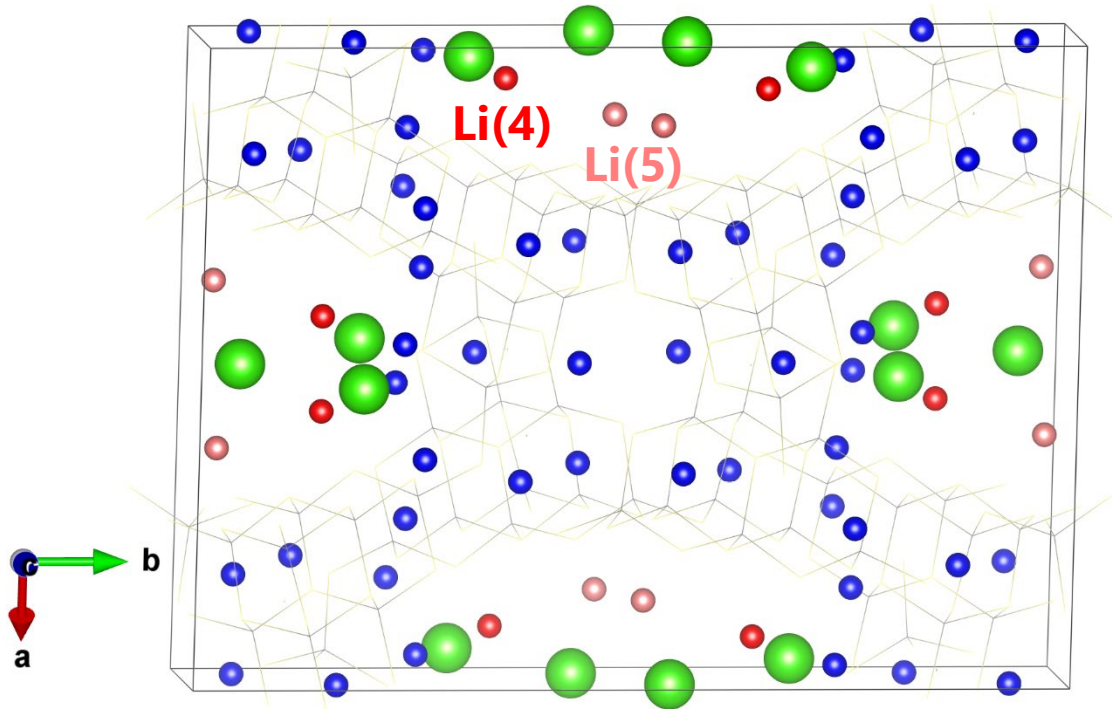

Visualization of active Li sites for

$Li_{7.5}B_{10}S_{18}X_{1.5}$ (X = Cl, Br, I)

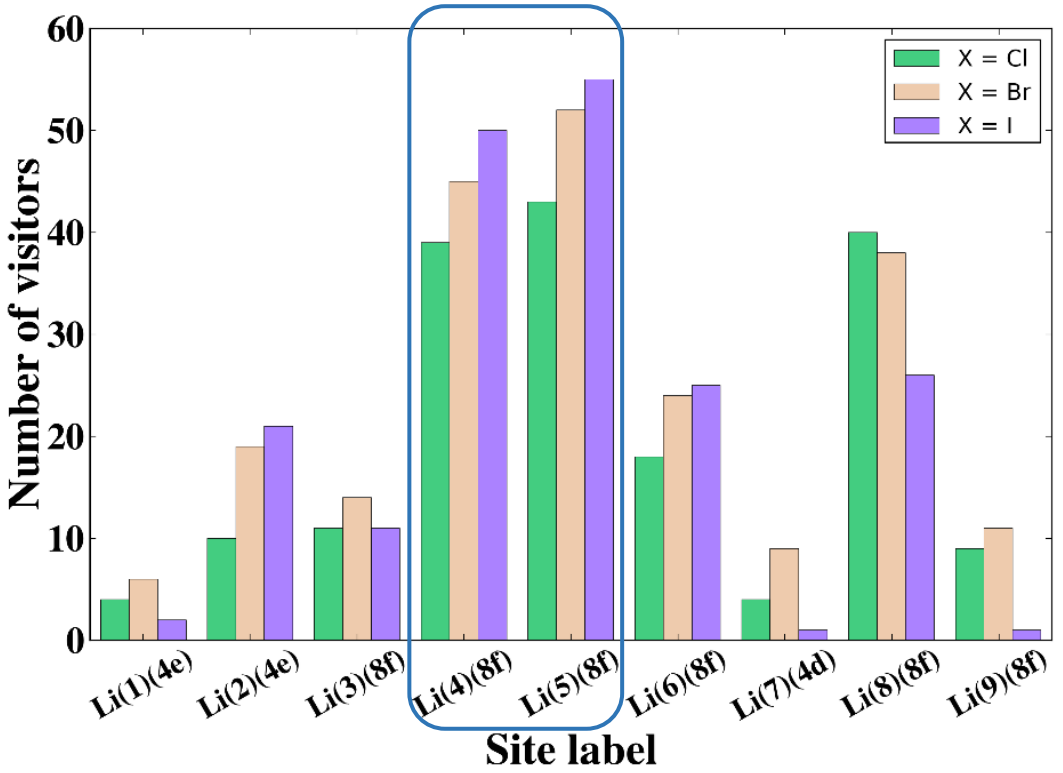

Number of visitors of each distinct Li site evaluated from MD simulation trajectories at 800 K

Summary of the project

- Computationally determined plausible idealized structures for the $Li_{7.5}B_{10}S_{18}X_{1.5}$ (X = Cl, Br, I) materials developed by Kaup *et al.* (2021), consistent with published X-ray and neutron diffraction analyses.
- Computed equilibrium total energies suggest chemical stability against decomposition.
- MD simulations show remarkable 3-dimensional Li ion mobility within the $B_{10}S_{18}$ framework at temperatures close to 400 K and higher.
- Preliminary analysis of detailed MD trajectories suggests concerted mechanisms for the Li ion motions primarily within the void cavities.

Manuscript in preparation

Resources of publications and presentations

http://users.wfu.edu/natalie/recentpubs.html

Link to Google Scholar Profile

Computational study of Li_3BO_3 and Li_3BN_2 I: Electrolyte properties of pure and doped crystals and II: Stability analysis of pure phases and of model interfaces with Li anodes
Yan Li, Zachary D. Hood, and N.A.W. Holzwarth
Physical Review Materials **5** , 085402 (2021) (I) and Physical Review Materials **5** , 085403 (2021) (II) Local copies: I and II

"Computational and experimental (re)investigation of the structural and electrolyte properties of $Li_4P_2S_6$, and $Na_4P_2S_6$, and $Li_2Na_2P_2S_6$"
Yan Li, Zachary D. Hood, and N.A.W. Holzwarth
Physical Review Materials **4** , 045406 (2020) Local copy

"Continuity of phonon dispersion curves in layered ionic materials "
Yan Li, W. C. Kerr, and N. A. W. Holzwarth
Journal of Physics: Condensed Matter **32** 055402 (2019) (local copy)

"Updated comments on projector augmented wave (PAW) implementations within various electronic structure code packages"
N. A. W. Holzwarth
Computer Physics Communications **234** 25-29 (2019) https://doi.org/10.1016/j.cpc.2019.05.009 (local copy)

http://users.wfu.edu/natalie/presentations.html

- Presentation by Yan Li at the 240th ECS Meeting Oct 10-14, 2021 -- "Computational Investigation of Li Boracite $Li_4B_7O_{12}Cl$ and Related Materials as Solid Electrolytes " (link to abstract)
- Presentation by N. A. W. Holzwarth at the 240th ECS Meeting Oct 10-14, 2021 -- "First Principles Simulations to Understand the Structural and Electrolyte Properties of Idealized $Li_{7.5}B_{10}S_{18}X_{1.5}$ (X = Cl, Br, I) -- Li Superionic Conductors Recently Identified in the Experimental Literature " (link to abstract)
- Presentation by N. A. W. Holzwarth at the Electronic Structure Discussion Group at Cambridge University invited by WFU alum Angela Harper -- June 9, 2021 -- First principles simulations of electrolyte materials with a view toward all solid-state battery technology -- $Li_4P_2S_6$, $Na_4P_2S_6$, and possible alloys
- Presentation by N. A. W. Holzwarth at the 10^{th} ABINIT International Developer Workshop May 31-June 4, 2021 -- Progress on self-consistent meta-gga PAW datasets from ATOMPAW (PP slides)
- Presentation by Yan Li at the March 2021 APS meeting -- "Li_3BO_3 and Li_3BN_2: Computational study of structural and electrolyte properties of pure and doped crystals" (link to abstract)
- Annotated slides that would have been presented by Yan Li at the cancelled March 2020 APS meeting -- "Prediction and analysis of a sodium ion electrolyte: $Li_2Na_2P_2S_6$"

Acknowledgements

10/21/2021

Photo taken at ECS meeting with → our experimental collaborator Dr. Zachary Hood (ANL) and Professor Natalie Holzwarth in Atlanta, GA in Oct. 2019

Thank you for your attending!